Half-sandwich complexes of osmium containing guanidine-derived ligands

Amie Parker, Pilar Lamata,* Fernando Viguri, Ricardo Rodríguez, José A. López, Fernando J. Lahoz, Pilar García-Orduña and Daniel Carmona*

Pyridinyl- and phosphano-guanidino complexes of formula $[(\eta^6\text{-}p\text{-}$ cymene)OsCl(**H₂L**)][SbF₆] (cymene = MeC₆H₄iPr; **H₂L** = N,N'-bis(p-Tolyl)-N''-(2-pyridinylmethyl)guanidine, **H₂L1** (**1**) and N,N'-bis(p-Tolyl)-N''-(2-diphenylphosphanoethyl)guanidine, **H₂L2** (**2**)) have been prepared from the dimer $[\{(\eta^6\text{-}p\text{-}$cymene)OsCl$\}_2(\mu\text{-}Cl)_2]$ and **H₂L** in the presence of NaSbF₆. Treatment of complex **2** with HCl renders the phosphano-guanidinium complex $[(\eta^6\text{-}p\text{-}$ cymene)OsCl₂(**H₃L₂**)][SbF₆] (**3**). Compounds **1** and **2** react with AgSbF₆ rendering the cationic aqua complexes $[(\eta^6\text{-}p\text{-}$cymene)Os(**H₂L**)(OH₂)][SbF₆]₂ (**H₂L** = **H₂L1** (**4**), **H₂L2** (**5**)). Addition of monodentate ligands **L** to compound **4** affords complexes of formula $[(\eta^6\text{-}p\text{-}$cymene)Os(**H₂L1**)L][SbF₆]₂ (**L** = py (**6**), 4-(NHMe)py (**7**), CO (**8**), P(OMe)₃ (**9**)). Treatment of complexes **4** and **5** with NaHCO₃ renders the monocationic complexes $[(\eta^6\text{-}p\text{-}$cymene)Os($\kappa^3N,N',N''$-**HL1**)][SbF₆] (**10**) and $[(\eta^6\text{-}p\text{-}$ cymene)Os(κ^3N,N',P-**HL2**)][SbF₆] (**11**), respectively, in which the **HL** ligand adopts a

----

Instituto de Síntesis Química y Catálisis Homogénea (ISQCH), CSIC - Universidad de Zaragoza, Departamento de Química Inorgánica, Pedro Cerbuna 12, 50009 Zaragoza, Spain
E-mail: dcarmona@unizar.es, plamata@unizar.es

fac-κ^3 coordination mode. The new complexes have been characterised by analytical and spectroscopic means, including the determination of the crystal structures of the

compounds **1-4**, **6**, **8**, **11**, by X-ray diffractometric methods. The phosphano-guanidino complexes **2** and **5** exhibit a temperature dependent fluxional process in solution. The new 18 electron complexes **1**, **2**, **6**, **8-10** are active catalyst for the Friedel-Crafts reaction between *trans-β*-nitrostyrene and *N*-methyl-2-methylindole. Conversions greater than 90 % were obtained. Proton NMR studies support a mechanism involving the Brønsted-acid activation of *trans-β*-nitrostyrene through the NH functionalities of the coordinated guanidine ligands.

Introduction

Guanidines and their derivatives are highly useful compounds that have found a large variety of applications in fields as diverse as catalysis,[1] coordination chemistry,[1b,2] materials science[1f,1i,2b,3] or biological and supramolecular chemistry.[2b,4] In particular, ligands containing the CN_3 guanidine moiety have been widely used for the stabilization of different metal complexes, taking advantage of their capability of bonding to the metals as neutral, monoanionic or dianionic ligands in a variety of coordination modes.[1b,2] However, osmium compounds with this class of ligands remain surprisingly rare. Thus, as far as we know, only the dinuclear complexes [Os₂Cl₂(hpp)₂]ⁿ, (n = 0, 1; hpp = the anion of 1,3,4,6,7,8-hexahydro-2*H*-pyrimido[1,2-*a*]pyrimidine),[5] the octahedral species [Os(Tpg)₂(CO)(PPh₃)], (HTpg = *N,N',N''*-triphenylguanidine)[6] and a family of half-sandwich complexes of formula [(η^6-*p*-cymene)OsCl(hpp)][7a] and [(η^6-*p*-cymene)OsCl{(C(NR)(N*i*Pr) NH*i*Pr)}][7b] have been reported so far.

On the other hand, the last decade has witnessed the development of organocatalysts based on weakly acidic molecules capable of acting as electrophile activators through either hydrogen bond or Brønsted acid catalysis.[8] The H-bond donating ability of these organic catalysts is usually enhanced by means of electron withdrawing substituents. Alternatively, this role has sometimes been played by metallic Lewis acids giving rise to Lewis acid assisted Brønsted acid (LBA) catalysts.[9] In the context of the present work, the contributions to this field of Meggers's and Gladysz's groups are particularly relevant. Meggers et al. have reported the application of octahedral 3-aminopyrazolato iridium(III) complexes as "metal-templated organocatalysts" to highly effective transfer hydrogenations, Friedel-Crafts reactions,

sulfa-Michael additions, *aza*-Henry reactions and α-amination of aldehydes.[10] Gladysz et al. have developed octahedral tris(chelate) cobalt complexes of ethylenediamines as hydrogen bond donors for promoting catalytic Michael additions, ring opening polymerization of lactide and additions of 1,3-dicarbonyl compounds.[11] Additionally, the latter group has also shown that half-sandwich ruthenium(II) complexes containing 2-guanidinebenzimidazole ligands are effective hydrogen bond donors that can catalyse the condensation of indoles and *trans*-β-nitrostyrene,[12] the ring opening polymerization of lactide[13] and the addition of malonate esters to nitroalkenes.[14] Finally, Mirkin et al. have demonstrated that hydrogen-bond-donating squaramide moieties within a Zr metal-organic framework and in a heteroligated Pt(II) complex catalyse the Friedel-Crafts reaction between indole and *trans*-β-nitrostyrene and that a functionalised biaryl urea group coordinated to Pt(II) catalyse the Diels-Alder reaction between cyclopentadiene and methyl vinyl ketone.[15]

In this regard, we have recently reported that water,[16] hydroxo-methylpyridine[17] or phosphano-hydroxo ligands[18] with an OH functionality coordinated to a Lewis acid metallic fragment can act as Brønsted acid electrophile activators for Friedel-Crafts and Diels-Alder reactions. Coordination to the metal enhances the acidity of the OH group of the ligand giving rise to LBA catalysts. As a continuation of this work, in the present paper, we report the preparation of the pyridinyl- and phosphano-guanidine ligands depicted in Scheme 1 with the aim of *i*) studying their coordination chemistry towards osmium and *ii*) applying the resulting complexes as LBA catalysts, through the NH functionalities present in the guanidine moiety of the ligands, in the Friedel-Crafts reaction between *trans*-β-nitrostyrene and *N*-methyl-2-dimethylindole.
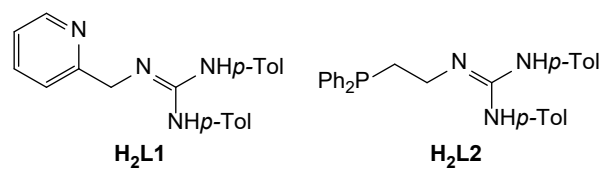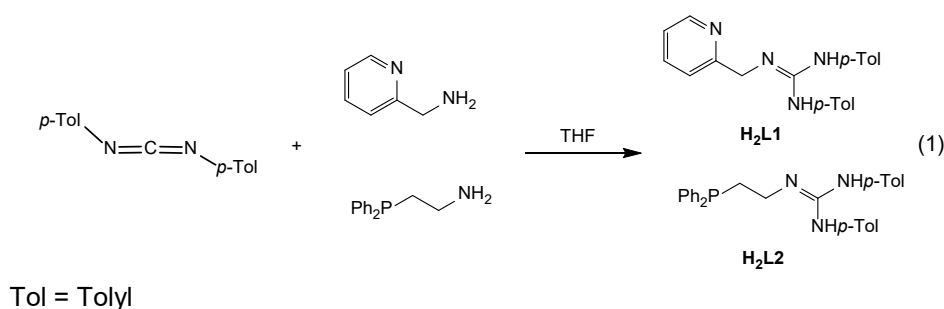
H₂L1

H₂L2

Tol = Tolyl

Scheme 1 Pyridinyl- and phosphano-guanidine ligands employed.

Results and discussion

Synthesis of the ligands

The ligands **H₂L1** and **H₂L2** have been prepared in high yield by reacting 1,3-disubstituted-carbodiimides with appropriately functionalised primary amines in dry THF (eqn (1)) following literature procedures (see Experimental section).[19]

Tol = Tolyl

Syntheses of the chlorido complexes [(η⁶-*p*-cymene)OsCl(H₂L)][SbF₆] (H₂L = H₂L1 (1), H₂L2 (2))

The chlorido complexes **1** and **2** were prepared by treating the dimer [{(η⁶-*p*-cymene)OsCl}₂(μ-Cl)₂]²⁰ with stoichiometric amounts of the corresponding ligand in methanol in the presence of NaSbF₆ (eqn (2)).
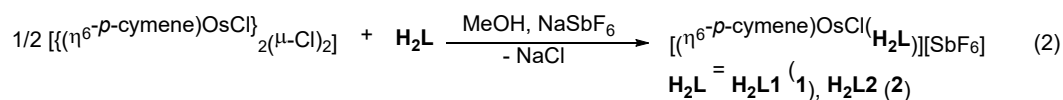
The complexes were characterized by analytical and spectroscopic means (see Experimental section). Assignment of the NMR signals was verified by two-dimensional homonuclear and heteronuclear correlations. Coordination of the pyridine nitrogen with the metal in complex **1** is supported by a strong deshielding of the H6 proton of the pyridine moiety, from 8.25 (free ligand) to 8.84 ppm (complex **1**). Similarly, a deshielding of about 40 ppm for the phosphorus nucleus indicates the

coordination of the phosphorus atom in complex **2**. Additionally, the plausible coordination of the iminic nitrogen in both complexes, forming a five-membered metallacycle, would render stereogenic the metal centre and diastereotopic the C−CH$_2$−N and P−CH$_2$−CH$_2$−N methylenes in complexes **1** and **2**, respectively (see Fig. 1). Indeed, these methylenes are asynchronous giving a pair of signals in each case and, therefore, supporting $\kappa^2 N,N'$ and $\kappa^2 N,P$ coordination modes for complexes **1** and **2**, respectively.

To unequivocally establish the solid state structure of the new species, the crystal structure of both compounds was determined by X-ray diffraction means. A view of the molecular structure of the cations is depicted in Fig. 1 and relevant characteristics of the metal coordination spheres are summarised in Table 1. Both complexes exhibit the so-called "three-legged piano-stool" geometry. An η^6-*p*-cymene group occupies three *fac* positions and the corresponding ligand, **H₂L1** (**1**) or **H₂L2** (**2**), occupies two coordination sites adopting a $\kappa^2 N,N'$ or $\kappa^2 N,P$ coordination mode. In both cases, the remaining coordination position is occupied by a chlorido ligand. The adopted pseudotetrahedral geometry renders the osmium a stereogenic centre.

Complex **1** crystallizes in the $P\bar{1}$ centrosymmetric space group and, therefore, the two enantiomers are present in the unit cell. However, complex **2** crystallizes in the chiral P2$_1$2$_1$2$_1$ space group as conglomerate and, according to the ligand priority sequence,[21] the absolute configuration of the measured crystal is *R* at osmium.
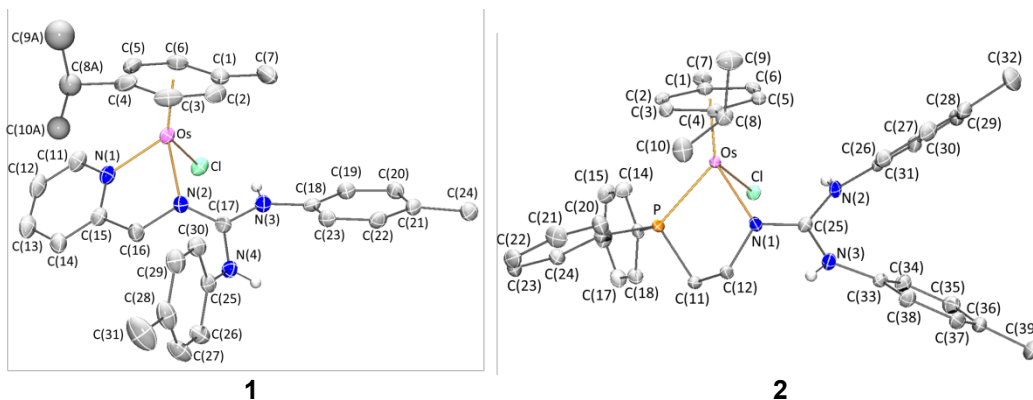
Fig. 1 Molecular structure of cation of complexes **1** and **2**. For clarity all the hydrogen atoms are omitted, except the N-H protons, and only the major component of the disordered *p*-cymene *i*Pr in complex **1** has been displayed.

Table 1 Selected bond lengths (Å) and angles (º) for complexes 1 and 2

Complex **1**				Complex **2**			
Os-Cl	2.4230(9)	Cl-Os-N(1)	84.02(9)	Os-Cl	2.4017(7)	Cl-Os-P	82.51(3)
Os-N(1)	2.092(3)	Cl-Os-N(2)	86.29(8)	Os-P	2.3289(8)	Cl-Os-N(1)	82.15(8)
Os-N(2)	2.106(3)	Cl-Os-Ct	128.12(7)	Os-N(1)	2.136(3)	Cl-Os-Ct^a	125.26(11)
Os-Ct^a	1.6759(2)	N(1)-Os-N(2)	76.58(12)	Os-Ct^a	1.7208(1)	P-Os-N(1)	81.29(8)
C(17)-N(2)	1.303(4)	N(1)-Os-Ct	132.05(11)	C(25)-N(1)	1.316(4)	P-Os-Ct^a	134.65(12)
C(17)-N(3)	1.361(4)	N(2)-Os-Ct	131.47(11)	C(25)-N(2)	1.361(4)	N(1)-Os-Ct^a	132.11(14)
C(17)-N(4)	1.372(4)			C(25)-N(3)	1.365(4)		

^{a} Ct stands for the centroid of the *p*-cymene ligand

From the determined bond distances and angles, there is no chemically significant difference to be remarked when comparing the two related complexes, **1** and **2**. Only the electronic situation of the central CN_3 guanidine carbon merits a comment. In particular, all the C−NH(*p*-Tolyl) bond distances are statistically identical (mean value: 1.365(2) Å), indicating a slightly partial double bond character for these bonds,[22] while the C−N bond distance involving the nitrogen coordinated to the metal atom is found to be comparatively shorter (1.303(4) (**1**) and 1.316(4) Å (**2**)), but always longer than typical N=C bond lengths (1.279(8) A).[22]
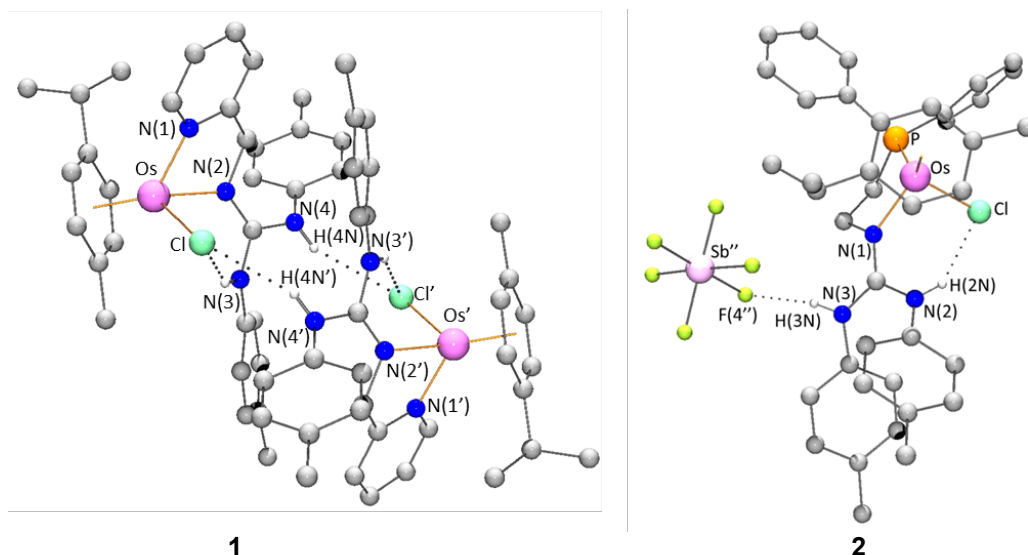
Fig. 2 Intra- and intermolecular interactions in complexes **1** and **2**. For clarity all the hydrogen atoms are omitted, except the N-H protons. Symmetry operations: i) 2-*x*, 2-*y*, 1-*z*; ii) -1 + *x*, *y*, *z*.

Analysis of the H-bond donating ability of N−H fragments points out the existence of similar N−H···Cl intramolecular interactions. However, in complex **1**, intermolecular N−H···Cl hydrogen bonds are observed between both enantiomers, leading to an $R_2^2(12)$ graphical set (Fig. 2). In complex **2**, the hydrogen atom of an NH fragment is involved in N−H···F interactions with a fluorine atom of the counterion. This kind of interaction will be also found in complexes **4**, **6** and **8** (vide infra).

Table 2 Geometrical parameters (Å, °) of H-bond interactions of complexes **1** and **2**

Complex	D-H···A	D-H	D···A	H···A	D-H···A
1	N(3)-H(3N)···Cl	0.85(2)	3.233(3)	2.47(2)	148(2)
1	N(4)-H(4N)···Cl'	0.85(3)	3.418(3)	2.62(3)	156(3)
2	N(2)-H(2N)···Cl	0.84(4)	3.297(3)	2.60(4)	140(3)
2	N(3)-H(3N)···F(4'')	0.84(4)	3.057(4)	2.27(4)	156(4)

Symmetry code: ') 2-*x*, 2-*y*, 1-*z*; '') -1+*x*, *y*, *z*

The NMR spectra of complex **1** do not change significantly from RT to 193 K. However, the ^{1}H NMR signals of complex **2** broaden as temperature decreases but no apparent split of these signals was observed even at 193 K. At this temperature, the ^{31}P{^{1}H} NMR spectrum of complex **2** showed two broad singlets centred at 21.3 and 22.1 ppm, in about 73/27 molar ratio, respectively, which coalesce to one unique sharp singlet at 19.93 ppm, by heating the sample to RT (Fig. 3a). These spectroscopic data suggest that complex **2** undergoes a fluxional process. The low temperature limiting

spectrum was achieved at 183 K and from the equilibration of the phosphorus nuclei, the free energy of activation, $\Delta G^{\#}$, at the coalescence temperature (208 K), for the process has been calculated: $\Delta G^{\#} = 9.28 \pm 0.12$ kcal·mol^{-1}.[23]

DFT calculations have been carried out to obtain information about the NMR behaviour observed in solution (see ESI). First, the structure found in the solid state for compound **2** (Fig. 1) and those of two of its isomers were considered. In the first isomer, labelled **2a**, a tautomer of the ligand forms a seven-membered metallacycle by adopting a $\kappa^2 N,P$ coordination mode, employing the nitrogen atom of one of the NHp-Tolyl groups; in the second, **2b**, the deprotonated ligand forms two metallacycles, one with five and the other with four members, by coordinating $\kappa^3 N,N',P$ using its three atoms with coordination capacity (Fig. 3b). DFT calculations established that the most stable isomer is compound **2**, the one found in the solid state and, the calculated relative energies for **2a** and **2b**, 13.7 and 22.6 kcal·mol^{-1}, respectively, are too high to be compatible with the molar ratio observed in NMR experiments. Then, we considered the δ/λ interconversion of the Os-P-C-C-N five-membered metallacycle. The calculated activation barrier for the interconversion is 7.3 kcal·mol^{-1}, smaller than that experimentally found (9.28 kcal·mol^{-1}) for the observed fluxional process. More importantly, the δ conformer (the one observed in the solid state) is 3.9 kcal·mol^{-1} more stable than the λ conformer and, therefore, the latter would not be observed in the NMR spectra. At this point, we realised that in the solid state structure of complexes **1** and **2** (Fig. 1), the NC(NHp-Tolyl)$_2$ moiety presents two different dispositions that can be characterized by the dihedral angle N(2)-C(17)-N(4)-C(25) = 49.3(5) º (complex **1**) and N(1)-C(25)-N(3)-C(33) = 152.2(3) º (complex **2**). These two dispositions define two rotamers. We envisaged that interconversion between the two involved rotamers for **2 (2 and 2c)** could account for the observed NMR behaviour in

this complex. Indeed, according to DFT calculations, **2** is only 0.1 kcal·mol^{-1} less stable than **2c** and the activation barrier **2c** → **2** was calculated as 9.4 kcal·mol^{-1} in good agreement with the $\Delta G^{\#}$ determined for the process (9.28 kcal·mol^{-1}) through NMR experimental data (Fig. 3c). In summary, we propose that complex **2** undergoes a fluxional process consisting of the interconversion between rotamers **2c**
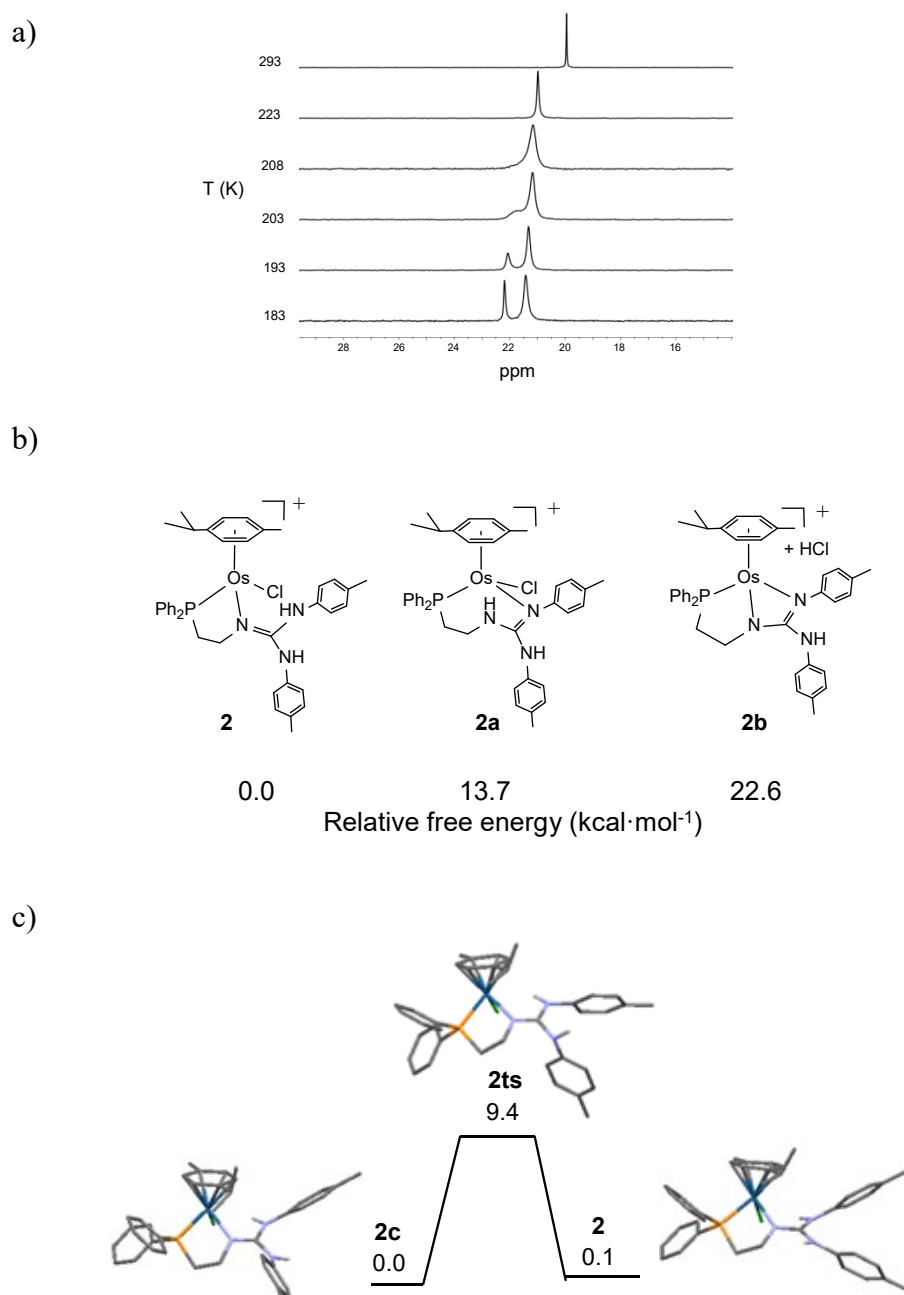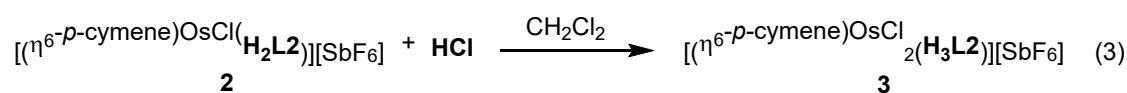
a)

b)

2	**2a**	**2b**
0.0	13.7	22.6

Relative free energy (kcal·mol^{-1})

c)

Fig. 3 a) Variation with temperature of the ^{31}P{^{1}H} NMR spectrum of complex **2** in CD$_2$Cl$_2$. b) Relative free energy for compounds **2**, **2a** and **2b.** c) Gibbs free energy profile of the equilibrium between rotamers **2c** and **2**. For clarity, except the NH protons, hydrogen atoms have been omitted. Free energies are in kcal·mol^{-1}.

and **2**. According to NMR data, this process is free at 283 K and is frozen at 183 K. The calculated barrier could be related to the partial double bond character encountered for the C−NH(*p*-Tolyl) bond (vide supra).

Synthesis of the complex [(η^6-*p*-cymene)OsCl$_2$(H$_3$L2)][SbF$_6$] (3)

When according to eqn (2), complex **2** was isolated in 96 % yield, two minor by-products were detected by NMR spectroscopy, each one in about 2 % abundance. One of them is complex **11** (see below) in which monodeprotonated **H$_2$L2** adopts a κ^3P,N,N' coordination mode with the osmium atom. An alternative preparation and the complete characterization of complex **11** will be discussed later. The other by-product, complex **3**, contains the protonated phosphane-guanidine **H$_3$L2** ligand. Complex **3** was independently prepared by treating complex **2** with a stoichiometric amount of HCl (eqn (3), see Experimental section).

$$[(\eta^{6}\text{-}p\text{-cymene})\text{OsCl}(\textbf{H}_2\textbf{L2})][\text{SbF}_6] \ + \ \textbf{HCl} \ \xrightarrow{\text{CH}_2\text{Cl}_2} \ [(\eta^{6}\text{-}p\text{-cymene})\text{OsCl}_2(\textbf{H}_3\textbf{L2})][\text{SbF}_6] \quad (3)$$

$$\textbf{2} \qquad\qquad\qquad\qquad\qquad\qquad\qquad\qquad\qquad\qquad \textbf{3}$$

As a result of the protonation of complex **2**, in the proton NMR spectrum of complex **3** are detected three singlets at 9.05, 6.77 and 5.88 ppm, which are attributed to the presence of three different NH protons in the molecule.

Notably, the phosphano-guanidino phosphorus nucleus of complex **3** resonates at -22.85 ppm, 42.78 ppm apart from the chemical shift observed for the same nucleus in complex **2**. This remarkable difference can be attributed to the "deshielding ring contribution" originated when a coordinated monodentate phosphane becomes part of a five-membered chelate ring.[24]
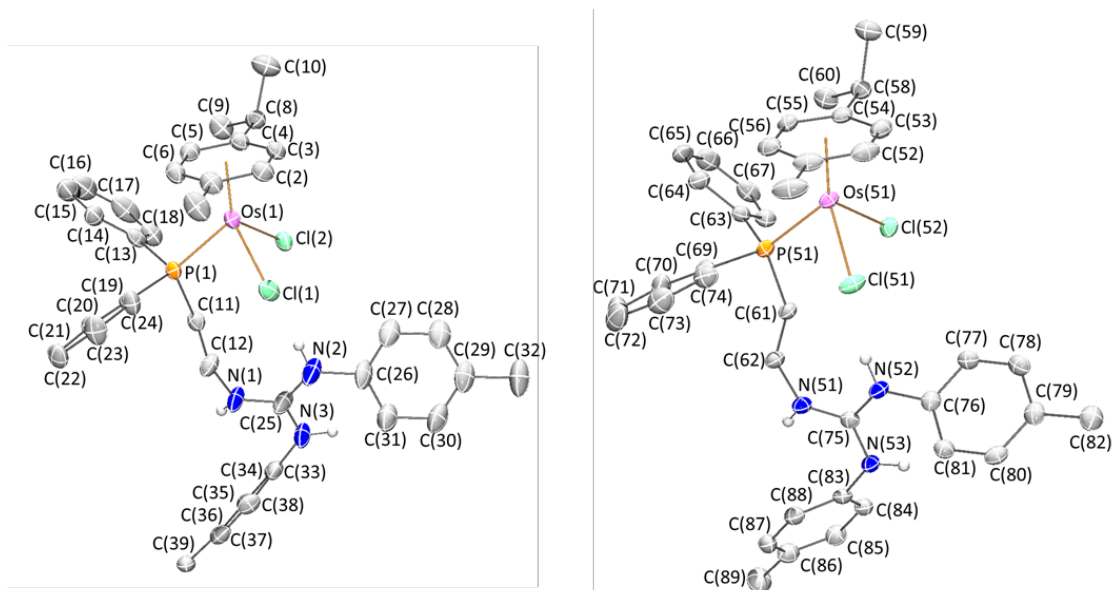
Fig. 4 Molecular structure of the two independent cations of complex **3**. For clarity all the hydrogen atoms are omitted except the NH protons.

The crystal structure of complex **3** has been determined by single crystal X-ray diffraction methods. Its asymmetric unit contains two crystallographically independent but chemically equivalent molecules; the molecular structure of both cations is shown in Fig. 4. Excepting the Os-Cl bond lengths, where statistical small differences are observed, all the rest of bond distances, in both independent molecules, are identical (Table 3). The most interesting feature is the presence of a planar $C(NH_3)$ guanidino carbon (Σ° C(25) = Σ° C75) = 360.0(7)$^\circ$) with equivalent C−N distances, all in the narrow range 1.326 to 1.351(5), confirming a similar partial double bond character for all the three CN bonds.

Table 3 Selected bonds lengths (Å) and angles (º) for both independent molecules of complex **3**

Os(1)-Cl(1)	2.4288(11)	Os(51)-Cl(51)	2.4187(10)
Os(1)-Cl(2)	2.4304(10)	Os(51)-Cl(52)	2.4302(10)
Os(1)-P(1)	2.3605(10)	Os(51)-P(51)	2.3611(11)
Os(1)-Ct(1)[a]	1.694(2)	Os(51)-Ct(51)[a]	1.6946(16)
C(25)-N(1)	1.330(6)	C(75)-N(51)	1.326(5)
C(25)-N(2)	1.343(7)	C(75)-N(52)	1.339(5)
C(25)-N(3)	1.338(6)	C(75)-N(53)	1.351(5)
Cl(1)-Os(1)-Cl(2)	85.29(4)	Cl(51)-Os(51)-Cl(52)	86.30(4)
Cl(1)-Os(1)-P(1)	89.90(4)	Cl(51)-Os(51)-P(51)	86.67(4)
Cl(1)-Os(1)-Ct(1)	125.23(8)	Cl(51)-Os(51)-Ct(51)	125.77(7)
Cl(2)-Os(1)-P(1)	86.67(3)	Cl(52)-Os(51)-P(51)	85.43(3)
Cl(2)-Os(1)-Ct(1)	126.23(7)	Cl(52)-Os(51)-Ct(51)	126.91(7)
P(1)-Os(1)-Ct(1)	129.77(8)	P(51)-Os(51)-Ct(51)	131.10(7)

[a] Ct stands for the centroid of the *p*-cymene ligand

Table 4 Geometrical parameters (Å, °) of the H-bond interactions of complex **3**

	N-H	H···A	N···A	N-H···A
N(1)-H(1N)···F(7)	0.86(3)	2.11(4)	2.931(6)	158(2)
N(51)-H(51N)···F(4)'	0.874(4)	2.272(4)	3.069(5)	151.6(2)
N(53)-H(53N)···Cl(52)''	0.86(3)	2.59(4)	3.386(4)	155(3)

In both independent molecules, a hydrogen bond between the CH_2NH proton and the SbF_6^- anion was observed (Table 4). Additionally, one of the independent molecules also shows a hydrogen bond between one of the NH(*p*-Tolyl) protons and one of the chlorido ligands bound to the osmium (Fig. 5).
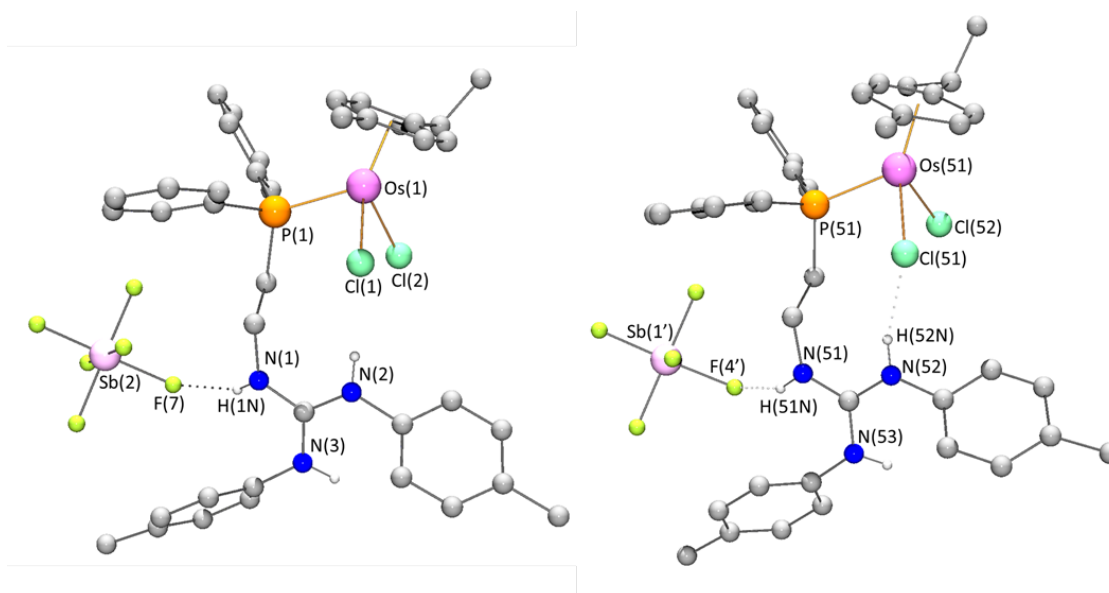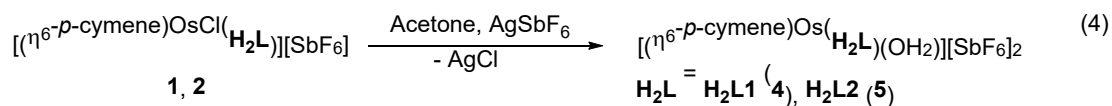

Fig. 5 View of the two independent molecules of complex **3** showing the detected hydrogen bonds. Primed atoms are related to non-primed ones through *x*, *y*-1, *z* symmetry operation.

Syntheses of the aqua-complexes [(η^6-*p*-cymene)Os(H₂L)(OH₂)][SbF₆]₂ (H₂L = H₂L1 (4), H₂L2 (5)

By treatment with $AgSbF_6$ in acetone, the chlorido ligand of complexes **1** and **2** was eliminated as AgCl. The presence of trace amounts of water in the solvents allows the isolation of the aqua-complexes [(η^6-*p*-cymene)Os(**H₂L**)(OH₂)][SbF₆]₂ (**H₂L** = **H₂L1** (**4**), **H₂L2** (**5**) in high yield (eqn (4)).

14

$$[(\eta^6\text{-}p\text{-cymene})OsCl(H_2L)][SbF_6] \xrightarrow[-\ AgCl]{Acetone,\ AgSbF_6} [(\eta^6\text{-}p\text{-cymene})Os(H_2L)(OH_2)][SbF_6]_2 \quad (4)$$

1, 2

$$H_2L = H_2L1\ (\mathbf{4}),\ H_2L2\ (\mathbf{5})$$

Complexes **4** and **5** were characterized by analytical and spectroscopic means (see Experimental section) and by the determination of the crystal structure of complex **4** by X-ray diffraction methods. As commented for complex **1**, in complex **4** a strong deshielding was also observed for the H6 proton of the pyridine moiety ($\delta(H_6Py)$ = 9.13 ppm). In both complexes, broad IR bands above 3100 cm^{-1} were attributed to the NH bonds present in the molecule. Fig. 6 shows a view of the molecular structure of the cation of compound **4** and the most relevant structural parameters are collected in Table 5.
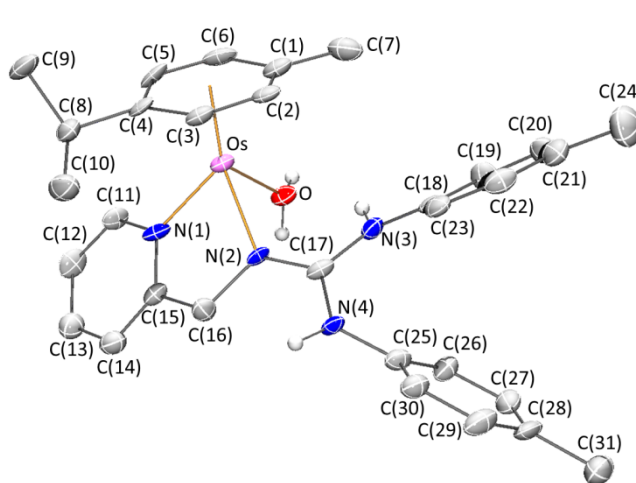

Fig. 6 Molecular structure of the cation of complex **4**. For clarity all the hydrogen atoms are omitted, except the water and NH protons.

Table 5 Selected bond lengths (Å) and angles (°) for complex **4**

Os-O	2.174(7)	O-Os-N(1)	82.7(3)
Os-N(1)	2.064(8)	O-Os-N(2)	79.7(3)
Os-N(2)	2.090(7)	O-Os-Ct^a	131.27(1)
Os-Ct^a	1.6726(15)	N(1)-Os-N(2)	76.8(3)
C(17)-N(2)	1.313(11)	N(1)-Os-Ct^a	131.69(1)
C17)-N(3)	1.356(13)	N(2)-Os-Ct^a	133.75(1)
C(17)-N(4)	1.363(11)		

^{a} Ct stands for the centroid of the *p*-cymene ligand

The half-sandwich complex **4** adopts a pseudotetrahedral piano-stool geometry with the osmium coordinated with the *p*-cymene ligand, the pyridinic and iminic nitrogens of the guanidine ligand and the oxygen atom of a water molecule. The osmium atom is a stereogenic centre and complex **4** crystallizes in the $P\bar{1}$ centrosymmetric space group as a racemate. Geometrical parameters of the metal coordination sphere agree with those found in complex **1**. Proton NH atoms are only involved in N−H⋯F interactions with one of the counterions (see Electronic Supplementary Information).

At 298 K, the proton and phosphorus NMR spectra of complex **5** consist of only one set of signals. However, these spectra are temperature dependent. In particular, the singlet of the $^{31}P\{^{1}H\}$ NMR spectrum at 298 K, upon cooling, broadens out, coalesces at about 277 K and splits into two differently populated signals (72/28 ratio) below this temperature (Fig. 7a). The low temperature limiting spectrum was achieved at 193 K and, from the equilibration of the phosphorus nuclei, the free energy of activation, $\Delta G^{\#}$, at the coalescence temperature, for the fluxional process has been calculated: $\Delta G^{\#} = 12.22 \pm 0.12$ kcal·mol^{-1}.[23] As for complex **2**, we suggest that the fluxional behaviour of complex **5** consists of the interconversion between two rotamers, **5c** and **5**, that can be characterised by the values of the dihedral angles involving the NC−(NH*p*-Tolyl)$_2$ core of the guanidino ligand (Fig. 7b). Indeed, a DFT study shows a difference of 0.4 kcal·mol^{-1} between the two rotamers with an activation barrier of 12.6 kcal·mol^{-1} for the **5c** → **5** process, in good agreement with the observed experimental NMR data (Fig. 7b).
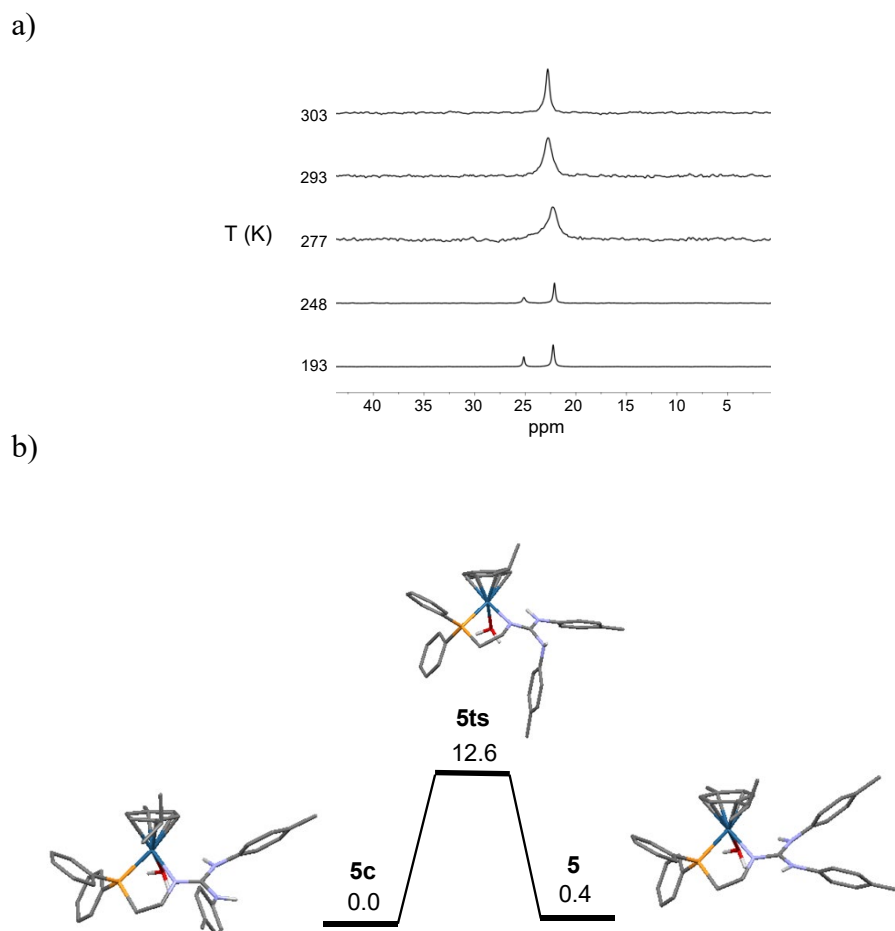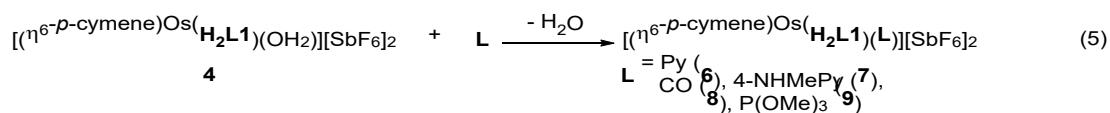
Fig. 7 a) Variation with temperature of the $^{31}P\{^1H\}$ NMR spectra of complex **5** in CD_2Cl_2. b) Gibbs free energy profile of the equilibrium between rotamers **5c** and **5**. For clarity, except the NH protons, hydrogen atoms have been omitted. Free energies are in kcal·mol^{-1}.

Syntheses of the cationic complexes $[(\eta^6\text{-}p\text{-cymene})Os(H_2L1)(L)][SbF_6]_2$ (L = Py (6), 4-NHMePy (7), CO (8), P(OMe)$_3$ (9))

Substitution of the coordinated water molecule in complex **4** by monodentate ligands such as, pyridine (Py), 4-methylamine pyridine (4-NHMePy), carbon monoxide or trimethylphosphite gives rise to the corresponding cationic complexes $[(\eta^6\text{-}p\text{-}$ cymene)Os(**H$_2$L1**)(L)][SbF$_6$]$_2$ (**L** = Py (**6**), 4-NHMePy (**7**), CO (**8**), P(OMe)$_3$ (**9**)) (eqn (5)).

$$[(\eta^{6}\text{-}p\text{-cymene})Os(\textbf{H}_2\textbf{L1})(OH_2)][SbF_6]_2 \;+\; \textbf{L} \;\xrightarrow{-\,H_2O}\; [(\eta^{6}\text{-}p\text{-cymene})Os(\textbf{H}_2\textbf{L1})(\textbf{L})][SbF_6]_2 \qquad (5)$$

4

L = Py (**6**), CO (**8**), 4-NHMePy (**7**), P(OMe)₃ (**9**)

The new compounds have been characterised by analytical and spectroscopic methods as well as by the determination of the crystal structure of complexes **6** and **8** by X-ray crystallography. Proton NMR data are compatible with a 1/1/1, *p*-cymene/**H₂L**/**L** molar ratio. In particular, the IR spectrum of compound **8** shows a band at 2024 cm⁻¹ attributed to the coordinated carbon monoxide and the $^{31}P\{^{1}H\}$ NMR spectrum of compound **9** consists of a singlet at 74.32 ppm due to the presence of coordinated trimethylphosphite.

A view of the molecular structure of the cations of compounds **6** and **8** is shown in Fig. 8. Tables 6 lists the most relevant structural features of the complex **6** and those of the two independent molecules encountered for complex **8**.
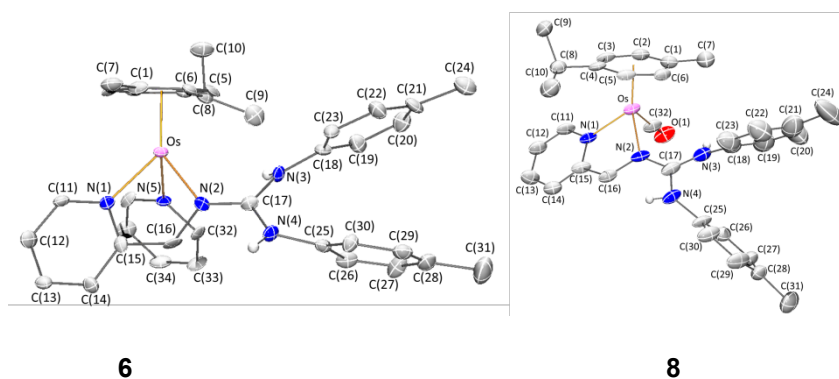

6   **8**

Fig. 8 Molecular structure of the cation of complexes **6** and **8**. For clarity all the hydrogen atoms are omitted, except the N−H protons.

Table 6 Selected bond lengths (Å) and angles (º) for complexes **6** and **8**

	6	8(1)	8(2)
Os-N(1)	2.102(9)	2.077(8)	2.083(8)
Os-N(2)	2.118(9)	2.098(7)	2.100(7)
Os-N(5)/C(32)[a]	2.144(9)	1.890(10)	1.904(11)
Os-Ct[b]	1.701(5)	1.7660(1)	1.7574(1)
N(1)-Os-N(2)	77.6(3)	77.1(3)	76.7(3)
N(1)-Os-N(5)/C(32)[a]	78.5(3)	88.6(4)	89.6(4)
N(1)-Os-Ct[b]	132.5(3)	127.60(1)	126.96(1)
N(2)-Os-N(5)/C(32)[a]	87.1(3)	93.3(3)	92.6(3)
N(2)-Os-Ct[b]	132.5(3)	127.91(1)	126.88(1)
N(5)/C(32)[a] -Os-Ct[b]	128.9(3)	127.18(1)	128.57(1)
C(17)-N(2)	1.321(14)	1.311(12)	1.320(12)
C(17)-N(3)	1.352(14)	1.350(15)	1.346(14)
C(17)-N(4)	1.363(14)	1.366(13)	1.357(12)

[a] N(5) in complex **6** and C(32) in complex **8**. [b] Ct stands for the centroid of the *p*-cymene ligand

The cationic complexes exhibit "three-legged piano-stool" geometry. An η^6-p-cymene group occupies three *fac* positions and the κ^2N,N' chelating **H2L1** ligand and the pyridine nitrogen atom (complex **6**) or the carbon atom of the CO molecule (complex **8**) complete the coordination sphere of the metal. The metal is a stereogenic centre and both complexes crystallize as racemate in the $P\bar{1}$ centrosymmetric space group. Bond lengths and angles characterising the metal coordination sphere compared well with those reported for complexes with κ^2N,N' coordination modes (compounds **1** and **4**). Moreover, N−H···F interactions, similar to those previously commented, have been found in the crystal packing of complexes **6** and **8** (Supplementary material).

Fluxional behaviour of the pyridinyl-guanidino complexes 1, 4, and 6-9

The ^{1}H NMR data recorded for the pyridinyl-guanidino complexes **1**, **4**, and **6-9** deserve some comments. As discussed before, the fluxionality observed for the phosphano-guanidino complexes **2** and **5** can be rationalised by assuming the exchange between two rotamers around the C−NH bond of the CN_3 moiety of the phosphano-guanidino ligand. Single-crystal X-ray diffractometric data indicated that

the double bond character of the CH_2N-C bond is weakened by delocalization of its electronic charge on the two remaining C−NH bonds of the guanidine group and, as a consequence, the C−NH bond distances reflect a partial double bond character. DFT calculations indicate that, for complexes **2** and **5**, the energy barrier for the rotation around the C−NH bond is accessible at room temperature.
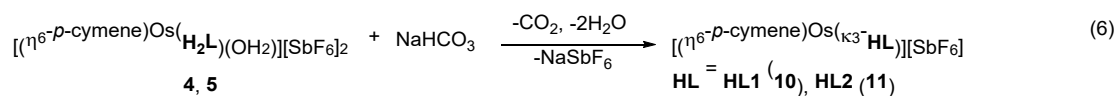
On the other hand, the structural data obtained by single-crystal X-ray methods for the pyridinyl-guanidino compounds **1**, **4**, **6** and **8** show that the C−NH bonds of the four complexes have a certain double bond character (see Tables 1, 5, and 6). Therefore, it can be expected that the guanidine core of complexes **1**, **4** and **6-9** also undergo a fluxional process similar to that described for complexes **2** and **5**. Support for this affirmation stems from the observation, at RT, of one set (complexes **4** and **6**, see Experimental section) or two sets (complexes **1**, **8** and **9**) of resonances for the guanidine NH(*p*-Tolyl) fragments of these complexes in their ^{1}H NMR spectra. It should be noted that detailed assignment of the proton NMR spectra is difficult due to the broadening and overlapping of some of signals.

In this regard, DFT calculations carried out for complex **1**, indicate that the activation barrier for the interconversion of two rotamers defined by the N(2)-C(17)-N(4)-C(25) dihedral angle (-44.5 º complex **1,** 154.6 º complex **1b**, see Figure 1 and ESI) is 9.5 kcal/mol, a value similar to that calculated for complex the phosphano-guanidino complex **2** (9.4 kcal·mol^{-1}, see above). However, whereas the energy difference between the two rotamers of complex **2** is only 0.1 kcal·mol^{-1} the energy difference between the corresponding rotamers of complex **1** is 2.5 kcal·mol^{-1} (see ESI). Therefore, the less stable rotamer of complex **1** would not be observable by proton NMR.

In summary, it can be anticipated that all the pyridinyl-guanidino complexes, **1**, **4** and **6-9**, undergo a fluxional process similar to that described before. The instability at temperatures above room temperature of the involved compounds and the strong broadening and signal overlapping observed in the ^{1}H NMR spectra have meant that we did not delve further into this study.

Syntheses of the complexes [(η^6-p-cymene)Os(HL)][SbF$_6$] (H$_2$L = H$_2$L1 (10), H$_2$L2 (11))

Deprotonation of the **H₂L** ligand of complexes **4** and **5** by NaHCO$_3$ renders the corresponding complexes [(η^6-p-cymene)Os(**HL**)][SbF$_6$] (**HL** = **HL1 (10)**, **HL2 (11)**) (eqn (6)) in which the **HL** ligand adopts a κ^3 coordination mode.

$$[(\eta^{6-p\text{-cymene}})Os(\mathbf{H_2L})(OH_2)][SbF_6]_2 \; + \; NaHCO_3 \; \xrightarrow[\text{-NaSbF}_6]{\text{-CO}_2, \text{-2H}_2O} \; [(\eta^{6-p\text{-cymene}})Os(_{\kappa 3^-}\mathbf{HL})][SbF_6] \qquad (6)$$

4, **5**　　　　　　　　　　　　　　　　　　　**HL** = **HL1** (**10**), **HL2** (**11**)

An IR band at 3359 and 3341 cm^{-1} for complexes **10** and **11**, respectively, and a singlet in the proton NMR spectrum at 6.15 and 5.76 ppm for **10** and **11**, respectively, are attributed to the remaining NH functionality. A peak at 23.87 ppm in the ^{31}P{^{1}H} NMR spectrum is assigned to the phosphorus nucleus of the PPh$_2$ group of complex **11**. As a reflect of the stereogenicity at the metal, the CH$_2$N methylene protons of complexes **10** and **11** are asynchronous. The molecular structure of complex **11**, determined by X-ray diffraction means (Fig. 9), reveals that the ligand **HL2** presents a *fac* $\kappa^3 N,N',P$ coordination mode that probably forces the central N(1) atom to adopt a pyramidal geometry (Σ angles around N(1) = 331.0(6) $^{\circ}$). This geometry contrasts with the sp^2 hybridization that this nitrogen atom presents when the **H₂L** ligands coordinate in a chelate $\kappa^2 N,P$ manner (compound **2**). The small N(1)-Os-N(2) and N(1)-C(25)-

N(2) angles, 61.85(17) and 109.1(4)º, respectively, far from the ideal hybridization values, reflect the strain of the four-membered metallacycle Os-N(1)-C(25)-N(2).
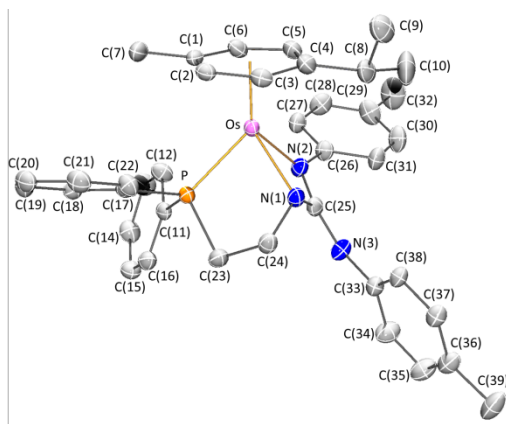

Fig. 9 Molecular structure of the cation of complex **11**. For clarity, all the hydrogen atoms are omitted.

Table 7 Selected bond lengths (Å) and angles (º) for complex **11**

Os-P	2.3302(12)	P-Os-N(1)	78.27(11)
Os-N(1)	2.134(4)	P-Os-N(2)	90.88(12)
Os-N(2)	2.107(4)	P-Os-Ct[a]	133.60(7)
Os-Ct[a]	1.703(2)	N(1)-Os-N(2)	61.85(17)
C(25)-N(1)	1.347(7)	N(1)-Os-Ct[a]	133.71(14)
C(25)-N(2)	1.329(7)	N(2)-Os-Ct[a]	131.38(14)
C(25)-N(3)	1.363(7)		

[a] Ct stands for the centroid of the *p*-cymene ligand

Catalytic reactions

Complexes **1**, **2**, **6** and **8-10** catalyse the Friedel-Crafts (FC) reaction between *N*-methyl-2-methylindole and *trans-β*-nitrostyrene. The coordinated water molecule of complexes **4** and **5** would be easily displaced by other ligands as it has been experimentally shown for complex **4** in the preparation of complexes **6-9**. To avoid the possible competence of Lewis acid catalysis, these two complexes have not been tested as catalysts in the FC reaction above mentioned. Table 8 gathers a selection of the obtained results together with the reaction conditions. The collected results are the average of at least two comparable reaction runs. Reactions were carried out in CH_2Cl_2, at 298 K. A molar ratio catalyst/nitroalkene/indole of 1/30/20 (5 mol %

catalyst loading) was employed in all cases. Reactions are clean: only the addition product and the remaining unreacted reagents were detected in the NMR spectra of the crude reaction mixture.

Table 8 Catalytic reaction of *N*-methyl-2-methylindole with *trans-β*-nitrostyrene[a]
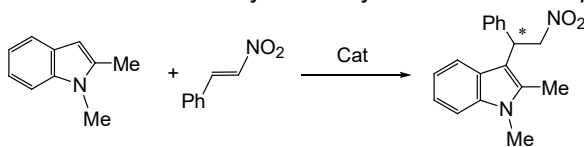
Entry	Catalyst	t (h)	Conv. (%)[b]
1	--	120	20
2	**H₂L1**	120	19
3	**H₂L2**	120	19
4	[(η^6-*p*-cymene)OsCl(**H₂L1**)][SbF₆] (**1**)	87	94
5	[(η^6-*p*-cymene)OsCl(**H₂L2**)][SbF₆] (**2**)	158	93
6	[(η^6-*p*-cymene)Os(**H₂L1**)(Py)][SbF₆]₂ (**6**)	6	95
7	[(η^6-*p*-cymene)Os(**H₂L1**)(CO)][SbF₆]₂ (**8**)	6	96
8	[(η^6-*p*-cymene)Os(**H₂L1**)(P(OMe)₃)][SbF₆]₂ (**9**)	48	94
9	[(η^6-*p*-cymene)Os(**HL1**)][SbF₆] (**10**)	48	90

[a] Reaction conditions: catalyst 0.03 mmol, *trans-β*-nitrostyrene (0.90 mmol), *N*-methyl-2-methylindole (0.60 mmol), in 2 mL of CH_2Cl_2. [b] Based on *N*-methyl-2-methylindole. Determined by NMR

All the complexes are active catalysts for the tested reaction. Whereas, in all cases, conversions greater than 90 % have been achieved after several hours of treatment, conversions lower than 20 % were attained after 120 hours of reaction using the free ligands as catalysts or in blank experiments. Dicationic complexes **6** and **8** are the most active catalysts. After only 6 hours of reaction, conversions of 95 and 96 %, respectively, were achieved. Most probably, Brønsted activation of the N−H bonds becomes more efficient when the charge of the molecule increases.

To shed light on the mechanism of the catalysis, solutions containing catalyst **9** and *trans-β*-nitrostyrene were monitored by NMR spectroscopy. Fig. 10 shows the evolution of a selected region of the ¹H NMR spectrum, by successive addition of *trans-β*-nitrostyrene to a CD₂Cl₂ solution of **9**. All proton resonances of **9** remain essentially unchanged but those of the NH protons. These resonances undergo a gradual
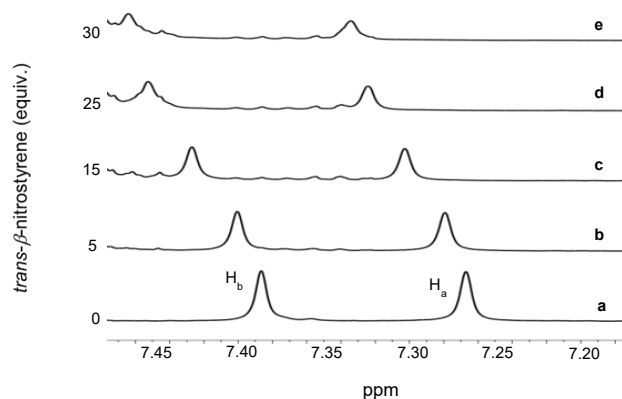
Fig. 10 Selected region of the ^{1}H NMR spectrum of the addition of *trans-β*-nitrostyrene to complex **9**: trace **a**, complex **9**; traces **b**, **c**, **d**, **e**, after the addition of 5, 15, 25 and 30 equiv. of *trans-β*-nitrostyrene, respectively.

downfield displacement from 7.27 ppm (H$_a$, see eqn (7)) and 7.39 ppm (H$_b$), (trace **a**, Fig. 10, δ values in the absence of *trans-β*-nitrostyrene) to 7.34 and 7.46 ppm, respectively (trace **e**, 30 equiv. of *trans-β*-nitrostyrene added). The NH protons shift can be accounted for by assuming that *trans-β*-nitrostyrene does not interact directly with the metal but an equilibrium between complex **9** and adduct **9a**, in which *trans-β*-nitrostyrene is hydrogen-bonded to the NH groups of **9**, is established in solution (eqn (7)). This interaction would be responsible for the activation of the electrophile in the FC catalytic reaction studied. Therefore, this process can be considered as an example of Brønsted-acid catalysis mediated by a Lewis acid assisted Brønsted-acid (LBA) catalyst.[9]
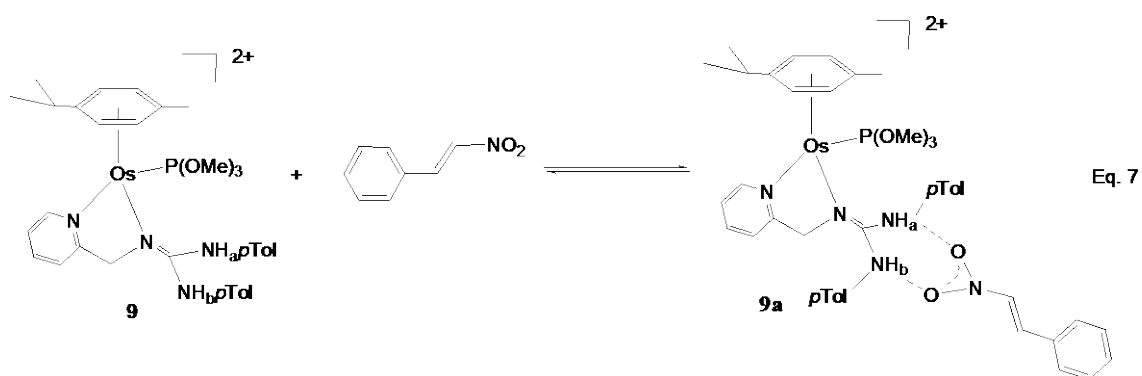
Conclusions

The pyridinyl- and phosphano-guanidine ligands **H₂L1** and **H₂L2** can form stable half-sandwich osmium complexes acting as κ^2N,N' or κ^2N,P ligands. The derived phosphano-guanidinium **H₃L2** cation coordinates as κ^1P ligand. Notably, the monodeprotonated guanidinato ligands **HL1** and **HL2** are able to form κ^3N,N',N'' or κ^3N,N',P chelates in which the hybridization of the central nitrogen atom have changed from sp^2 to sp^3 with the concomitant formation of a highly strained four-membered Os−N−C−N metallacycle. The new complexes catalysed the FC reaction between *trans-β*-nitrostyrene and *N*-methyl-2-methylindole. From spectroscopic data, it can be inferred that the complexes act as Brønsted-acid catalysts through the protons of the NH groups of the coordinated **H₂L** ligands. The findings reported herein may contribute to the development of new metal-containing Brønsted-acid catalysts in which the Brønsted acidity relies on M–XH functionalities.

Experimental

General information

All preparations have been carried out under argon. All solvents were treated in a PS-400-6 Innovative Technologies Solvent Purification System (SPS) and degassed prior to use. Infrared spectra were recorded on Perkin-Elmer Spectrum-100 (ATR mode) FT-IR spectrometer. Carbon, hydrogen and nitrogen analyses were performed using a Perkin-Elmer 240 B microanalyser. ^{1}H, ^{13}C and ^{31}P NMR spectra were recorded on a Bruker AV-300 spectrometer (300.13 MHz), Bruker AV-400 (400.16 MHz) or Bruker AV-500 (500.13 MHz). In both ^{1}H NMR and ^{13}C NMR measurements the chemical shifts are expressed in ppm downfield from $SiMe_4$. The ^{31}P NMR chemical shifts are relative to 85 % H_3PO_4. *J* values are given in Hz. NOESY and ^{13}C, ^{31}P and ^{1}H correlation spectra were obtained using standard procedures. Mass spectra were obtained with a Micro Tof-Q Bruker Daltonics spectrometer.

Preparation of the guanidine ligands H₂L1 and H₂L2

At RT, a mixture of 2-pyridinylmethanamine or 2-(diphenylphosphino)ethylamine (1.8 mmol) and 1,3-di-*p*-toyldicarbodimide (412.8 mg, 1.8 mmol) in dry THF (10 mL) was stirred for 15 h. The resulting solution was vacuum-evaporated to dryness. The residue was washed with hexane (3 × 5 mL). Evaporation of the solvent under vacuum gave the guanidine compounds as a white oil. Yield: 85 % (**H₂L1**), 88 % (**H₂L2**).
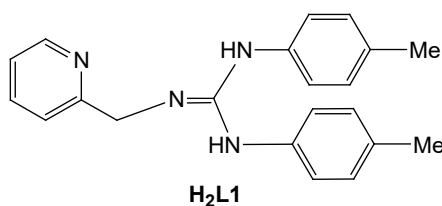
H₂L1

H₂L1. HRMS (*μ*-TOF), $C_{21}H_{22}N_4$, $[M + H]^+$, calcd: 331.1917, found: 331.1932. ^1H NMR (500.10 MHz, CD_2Cl_2, RT): δ = 8.25 (bd, *J*(H₅Py,H₆Py) = 7.7 Hz, 1H, H₆ Py), 7.68 (t, *J*(H₃Py,H₄Py) ≈ *J*(H₅Py,H₄Py) = 7.7 Hz, 1H, H₄ Py), 7.30 (d, *J*(H₄Py,H₃Py) = 7.7 Hz, 1H, H₃ Py), 7.20 (bt, *J*(H₄Py,H₅Py) ≈ *J*(H₆Py,H₅Py) = 7.7 Hz, 1H, H₅ Py), 7.11 (d), 6.98 (bs) (AB system, *J*(A,B) = 7.9 Hz, 8H, Ar), 5.25 (bs, 2H, NH), 4.56 (bs, 2H, CH₂), 2.30 (s, 6H, Me). $^{13}C\{^1H\}$ NMR (125.77 MHz, CD_2Cl_2, RT): δ = 159.10 (C₂(Py)), 149.69 (C₆(Py)), 149.39 (C=N), 137.47 (C₄(Py)), 130.65, 123.47 (Ar), 122.96 (C₅(Py)), 122.78 (C₃(Py)), 47.95 (CH₂), 21.29 (2 × Me).
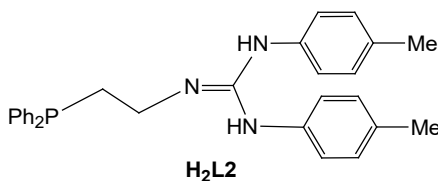

H₂L2

H₂L2. HRMS (*μ*-TOF), $C_{29}H_{30}N_3P$, $[M + H]^+$, calcd: 452.2250, found: 452.2264. ^1H NMR (300.10 MHz, $CDCl_3$, RT): δ = 7.45 - 7.30 (m, 10H, PPh₂), 7.08, 6.90 (AB system, *J*(A,B) = 9.0 Hz, 8H, Ar), 5.63 (bs, 1H, NH), 4.27 (bs, 1H, NH), 3.44 (m, 2H, NCH₂), 2.40 (m, 2H, PCH₂), 2.30 (s, 6H, Me). $^{13}C\{^1H\}$ NMR (100.62 MHz, $CDCl_3$, RT): δ = 149.70 (C=N), 138.03, 130.22 (Ar), 132.86 (d, *J*(P,C) = 18.8 Hz), 128.87, 128.67 (d, *J*(P,C) = 6.8 Hz), 128.87 (PPh₂), 39.57 (CH₂N), 28.70 (d, *J*(P,C) = 13.2 Hz, CH₂P), 20.88 (2 × Me). $^{31}P\{^1H\}$ NMR (202.46 MHz, $CDCl_3$, RT): δ = -20.96 (s).

Preparation of the complexes [(η^6-*p*-cymene)OsCl(H₂L)][SbF₆] (H₂L = H₂L1 (1), H₂L2 (2)

To a suspension of the dimer [{(η^6-*p*-cymene)OsCl}₂(*μ*-Cl)₂] (395.3 mg, 0.5 mmol), in methanol (10 mL), 1.0 mmol of **H₂L** and 258.7 mg (1.0 mmol) of $NaSbF_6$ were added. The resulting solution was stirred for 5 h and vacuum-evaporated to dryness. The

residue was extracted with dichloromethane and the solution was concentrated under reduced pressure to *ca.* 2 mL. The slow addition of hexane led to the precipitation of a yellow solid which was washed with hexane (3 × 10 mL) and vacuum-dried. Crystals of **1** and **2** suitable for X-ray diffraction analysis were obtained by crystallisation from CH₂Cl₂/methanol (**1**) or CH₂Cl₂/hexane (**2**) solutions.

1
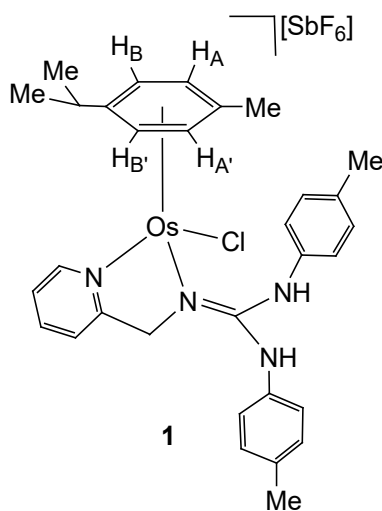
Complex 1. Yield: 868.6 mg, 94 %. Anal. Calcd for C₃₁H₃₆N₄ClF₆OsSb: C, 40.2; H, 3.9; N, 6.05. Found: C, 40.0; H, 3.8; N, 6.0. HRMS (*μ*-TOF), C₃₁H₃₆N₄ClF₆OsSb, [M−SbF₆]⁺, calcd: 691.2228, found: 691.2253. IR (cm⁻¹): 3303 (br), *v*(NH); 1623 (m), *v*(N=C, Py); 1608 (m), *v*(N=C); 653 (s), *v*(SbF₆). ¹H NMR (500.10 MHz, CD₂Cl₂, RT): δ = 8.84 (bd, *J*(H₅Py,H₆Py) = 7.4 Hz, 1H, H₆ Py), 8.34 (s, 1H, NH *trans* CH₂), 7.84 (t, *J*(H₃Py,H₄Py) ≈ *J*(H₅Py,H₄Py) = 7.5 Hz, 1H, H₄ Py), 7.41 (bd, *J*(H₄Py,H₃Py) = 7.5 Hz, 1H, H₃ Py), 7.39 (t, *J*(H₄Py,H₅Py) ≈ *J*(H₆Py,H₅Py) = 7.4 Hz, 1H, H₅ Py), 7.13 (s, 1H, NH *trans* Os), 7.02, 6.89 (AB system, *J*(A,B) = 8.3 Hz, 4 H, Ar), 6.99, 6.92 (AB system, *J*(A,B) = 8.3 Hz, 4 H, Ar), 5.95 (d, *J*(Hₐ',H_B') = 5.35 Hz, 1H, H_B'), 5.81 (d, *J*(H_B,Hₐ) = 5.7 Hz, 1H, Hₐ), 5.76 (d, 1H, H_B), 5.64 (d, 1H, Hₐ'), 5.25 (A part of an AB system, *J*(H_pro-S,H_pro-R) = 17.5 Hz, 1H, *H_pro-R*, CH₂), 4.87 (B part of an AB system, 1H, *H_pro-S*, CH₂), 2.50 (spt, 1H, CH *i*Pr), 2.21, 2.20 (2 × s, 6H, Me *p*-Tol), 2.15 (s, 3H,

Me *p*-cymene), 1.11, 1.09 (2 × d, *J*(H,H) = 7.0 Hz, 6H, Me *i*Pr). ^{13}C{^{1}H} NMR (125.77 MHz, CD$_2$Cl$_2$, RT): δ = 162.00, 154.63, 140.22, 126.32, 121.43 (Py), 154.37 (C=N), 136.35, 136.19, 134.77, 134.48, 130.93, 130.48, 120.79, 120.06 (Ar), 97.38 (*C*−Me *p*-cymene), 91.01 (*C*−*i*Pr *p*-cymene), 78.77 (CH$_A$), 75.80 (CH$_{A'}$), 75.62 (CH$_B$), 73.38 (CH$_{B'}$), 61.64 (CH$_2$), 32.16 (CH, *i*Pr), 23.48, 22.18 (Me *i*Pr), 21.19 ((Me *p*-Tol), 19.07 (Me *p*-cymene).


2
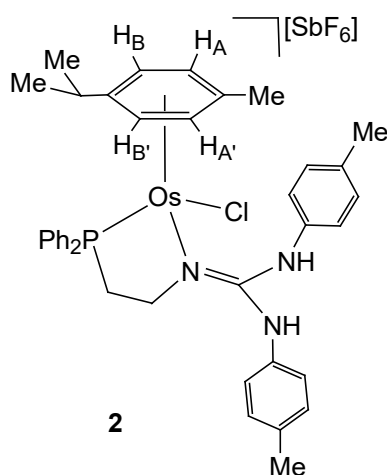
Complex 2. Yield: 1005.3 mg, 96 %. Anal. Calcd for C$_{39}$H$_{44}$N$_3$ClF$_6$OsPSb: C, 44.7; H, 4.2; N, 4.0. Found: C, 44.9; H, 4.2; N, 4.1. HRMS (*μ*-TOF), C$_{39}$H$_{44}$N$_3$ClF$_6$OsPSb, [M−SbF$_6$]$^+$, calcd: 812.2562, found: 812.2594. IR (cm^{-1}): 3135-3440 (br), ν(NH); 1608 (m), ν(N=C); 655 (s), ν(SbF$_6$). ^{1}H NMR (500.10 MHz, CD$_2$Cl$_2$, RT): δ = 8.71 (s, 1H, NH *trans* CH$_2$), 7.22 (s, 1H, NH *trans* Os), 7.70 - 7.30 (m, 10H, PPh$_2$), 7.04, 6.87 (AB system, *J*(A,B) = 8.3 Hz, 4 H, Ar), 7.00, 6.91 (AB system, *J*(A,B) = 8.3 Hz, 4 H, Ar), 5.81 (d, *J*(H$_B$,H$_A$) = 5.7 Hz, 1H, H$_A$), 5.77 (d, *J*(H$_{A'}$,H$_{B'}$) = 5.9 Hz, 1H, H$_{B'}$), 5.21 (d, 1H, H$_B$), 5.10 (d, 1H, H$_{A'}$), 4.28 (dm, *J*(P,H) = 40.8 Hz, 1H, H$_{pro-R}$ NCH$_2$), 3.38 (m, 1H, H$_{pro-S}$ NCH$_2$), 3.03 (m, 1H, H$_{pro-R}$ PCH$_2$), 2.29 (spt, 1H, CH *i*Pr), 2.23 (m, 1H, H$_{pro-S}$ PCH$_2$), 2.23, 2.22 (2 × s, 6H, Me *p*-Tol), 2.05 (s, 3H, Me *p*-cymene), 1.21, 1.06 (2 × d, *J*(H,H) = 6.9 Hz, 6H, Me *i*Pr). ^{13}C{^{1}H} NMR (125.77 MHz, CD$_2$Cl$_2$, RT): δ = 156.10 (C=N), 136.61, 136.47, 134.59, 134.21,

131.10, 130.50, 120.38, 119.13, 135.90 (d, J(P,C) = 55.11 Hz), 128.42 (d, J(P,C) = 61.74 Hz) (Ar), 103.38 (C−Me, p-cymene), 93.38 (C−iPr, p-cymene), 88.56 (CH$_{A'}$), 81.89 (CH$_B$), 81.13 (CH$_A$, CH$_{B'}$), 57.50 (CH$_2$N), 31.70 (d, J(P,C) = 33.8 Hz, CH$_2$P), 31.16 (CH, iPr), 23.16, 22.98 (Me iPr), 21.21, 21.18 (2 × Me p-Tol), 18.16 (Me, p-cymene). ^{31}P{^{1}H} NMR (202.46 MHz, CD$_2$Cl$_2$, RT): δ = 19.93 (s).

^{1}H NMR (500.10 MHz, CD$_2$Cl$_2$, 183 K): Major isomer: δ = 8.40 (s, 1H, NH $trans$ CH$_2$), 4.36 (dm, J(P,H) = 41.2 Hz, 1H, H$_{pro-R}$ NCH$_2$), 3.39 (m, 1H, H$_{pro-S}$ NCH$_2$), 3.09 (m, 1H, H$_{pro-R}$ PCH$_2$), 2.34-2.10 (2H, CH iPr, H$_{pro-S}$ PCH$_2$), 2.14, 2.10 (2 × bs, 6H, Me p-Tol), 1.95 (bs, 3H, Me p-cymene), 1.20-0.80 (2 × bs , 6H, Me iPr). Minor isomer: δ = 8.63 (s, 1H, NH $trans$ CH$_2$), 3.68 (dm, J(P,H) = 41.2 Hz, 1H, H$_{pro-R}$ NCH$_2$), 2.96 (m, 1H, H$_{pro-S}$ NCH$_2$), 2.78 (m, 1H, H$_{pro-R}$ PCH$_2$), 2.34, 2.25 (2 × bs, 6H, Me p-Tol), 2.34-2.10 (2H, CH iPr, H$_{pro-S}$ PCH$_2$), 1. 95 (bs, 3H, Me p-cymene), 1.20-0.80 (2 × bs, 6H, Me iPr). ^{31}P{^{1}H} NMR (202.46 MHz, CD$_2$Cl$_2$, 183 K): Major isomer: δ = 21.42 (s); minor isomer: δ = 22.19 (s).

Preparation of the complex [(η^6-p-cymene)OsCl$_2$(H$_3$L2)][SbF$_6$] (3)

To a solution of the complex [(η^6-p-cymene)OsCl(**H$_2$L2**)][SbF$_6$] (**2**) (20 mg, 0.019 mmol) in dichloromethane (2 mL), aqueous HCl (0.019 mmol) was added. The resulting solution was stirred for 5 days and concentrated under reduced pressure to *ca.* 0.5 mL. The slow addition of hexane led to the precipitation of a yellow solid which was washed with hexane (3 × 1 mL) and vacuum-dried. Crystals of **3** suitable for X-ray diffraction analysis were obtained by crystallisation from CH$_2$Cl$_2$/hexane solutions.
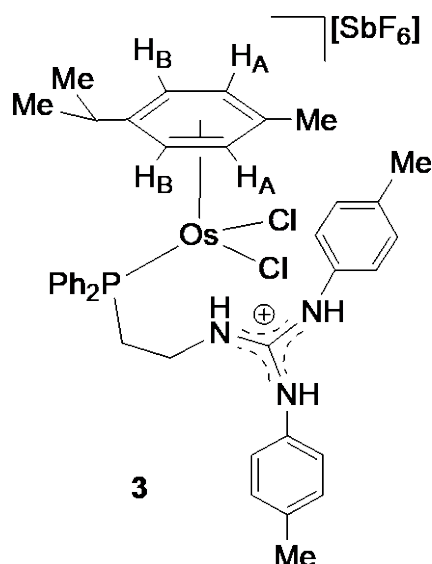
Complex 3. Yield: 12.0 mg, 60 %. Anal. Calcd for $C_{39}H_{45}N_3Cl_2F_6OsPSb$: C, 43.2; H, 4.2; N, 3.9. Found: C, 43.2; H, 4.4; N, 3.7. HRMS (μ-TOF), $C_{39}H_{45}N_3Cl_2F_6OsPSb$, $[M-SbF_6]^+$, calcd: 848.2319, found: 848.2355. IR (cm^{-1}): 3465-3120 (br), ν(NH); 1632, 1599 (m), ν(N=C); 654 (s), ν(SbF$_6$). ^{1}H NMR (500.10 MHz, CD$_2$Cl$_2$, RT): δ = 9.05 (bs, 1H, NH), 7.68-7.13 (m, 18H, Ar), 6.77 (bs, 1H, NH), 5.88 (bs, 1H, N*H*CH$_2$), 5.40 (d, J(H$_B$,H$_A$) = 5.7 Hz, 2H, H$_A$), 5.34 (d, 2H, H$_B$), 3.45 (m, 2H, CH$_2$N), 3.15 (m, 2H, CH$_2$P), 2.35 (bs, 6H, Me *p*-Tol), 2.30 (spt, 1H, CH *i*Pr), 2.00 (s, 3H, Me *p*-cymene), 1.04 (d, J(H,H) = 6.9 Hz, 6H, Me *i*Pr). ^{13}C{^{1}H} NMR (125.77 MHz, CD$_2$Cl$_2$, RT): δ = 154.19 (C=N), 134.00-129.50 PPh$_2$), 131.87, 127.21 (Ar), 101.55 (*C*−*i*Pr), 90.07 (*C*−Me *p*-cymene), 82.28 (CH$_A$), 80.18 (CH$_B$), 38.99 (CH$_2$N), 30.86 (CH *i*Pr), 26.84 (d, J(P,C) = 29.7 Hz, CH$_2$P), 22.66 (Me *i*Pr), 21.62 (2 × Me, *p*-Tol), 18.17 (Me *p*-cymene). ^{31}P{^{1}H} NMR (202.46 MHz, CD$_2$Cl$_2$, RT): δ = -22.85 (s).

Preparation of the complexes [(η^6-*p*-cymene)Os(H₂L)(OH₂)][SbF₆]₂ (H₂L = H₂L1 (4), H₂L2 (5)

To a solution of the corresponding chlorido complex **1** or **2** (0.30 mmol) in acetone (10 mL), 103.1 mg (0.3 mmol) of AgSbF₆ were added. The resulting suspension was stirred for 2 h. The AgCl formed was separated with cannula and the filtrate was concentrated under reduced pressure to *ca*. 2 mL. The slow addition of hexane led to the precipitation of a yellow solid, which was washed with hexane (3 × 5 mL) and vacuum-dried. Crystals of **4** suitable for X-ray diffraction analysis were obtained by crystallisation from CH₂Cl₂/hexane solutions.

4
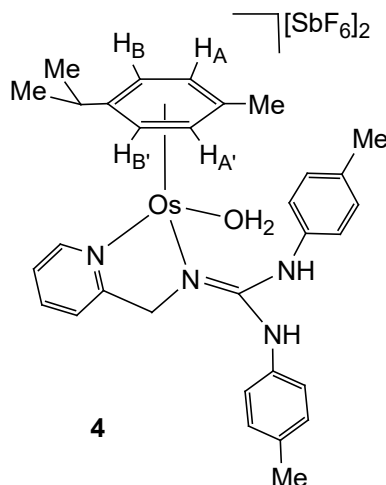
Complex 4. Yield: 1098.6 mg, 96 %. Anal. Calcd for C₃₁H₃₈N₄F₁₂OOsSb₂: C, 32.5; H, 3.35; N, 4.9. Found: C, 32.45; H, 3.1; N, 4.9. HRMS (*μ*-TOF), C₃₁H₃₈N₄F₁₂OOsSb₂, [M−2SbF₆−H₂O−H]⁺, calcd: 655.2480, found: 655.2472. IR (cm⁻¹): 3400 (br), *v*(NH); 3380 (m), *v*(OH); 1610(m), *v*(N=C); 653, *v*(SbF₆). ¹H NMR (500.10 MHz, CD₂Cl₂, RT): δ = 9.13 (bd, *J*(H₅Py,H₆Py) = 7.7 Hz, 1H, H₆Py), 7.95 (t, *J*(H₄Py,H₅Py) ≈ *J*(H₆Py,H₅Py) = 7.7 Hz, 1H, H₅Py), 7.52 (t, *J*(H₃Py,H₄Py) ≈ *J*(H₅Py,H₄Py) = 7.8 Hz, 1H, H₄Py), 7.50 (bd, *J*(H₄Py,H₃Py) = 7.8 Hz, 1H, H₃Py), 7.12 (s, 2H, NH), 7.04, 6.97 (AB system, *J*(A,B) = 8.3 Hz, 8H, Ar), 6.12 (m, 4H, H$_A$, H$_B$, H$_{A'}$, H$_{B'}$), 5.03 (brs, 2H, CH₂), 2.35 (spt, 1H, CH *i*Pr), 2.23 (s, 6H, Me *p*-Tol), 2.15 (s,

3H, Me), 1.06 (d, J(HH) = 6.9 Hz, 6H, Me iPr). ^{13}C{^{1}H} NMR (125.77 MHz, CD$_2$Cl$_2$,

RT): δ = 163.36, 154.76, 141.82, 127.26, 122.40 (Py), 156.36 (C=N), 135.96, 135.45,

130.91, 121.57 (Ar), 94.32, 90.99 (C−Me, C−iPr p-cymene), 77.37 (CH$_A$, CH$_B$, CH$_{A'}$,

CH$_{B'}$), 61.84 (CH$_2$), 32.00 (CH, iPr), 23.19, 23.04 (Me iPr), 21.28 (Me p-Tol, Me p-

cymene).

5
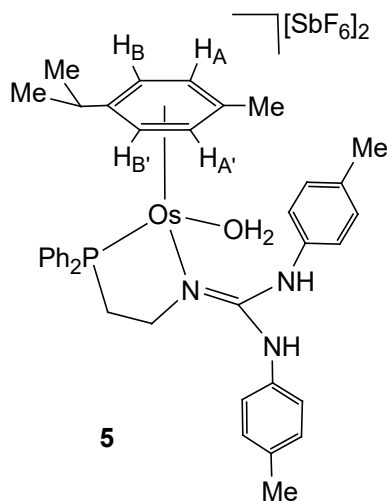
Complex 5. Yield: 1088.3 mg, 86 %. Anal. Calcd for C$_{39}$H$_{46}$N$_3$F$_{12}$OOsPSb$_2$: C,

37.0; H, 3.7; N, 3.3. Found: C, 36.9; H, 3.6; N, 3.2. HRMS (μ-TOF),

C$_{39}$H$_{46}$N$_3$F$_{12}$OOsPSb$_2$, [M−2SbF$_6$−H$_2$O−H]$^+$, calcd: 776. 2833 found: 776.2806. IR

(cm^{-1}): 3120-3330 (br), v(NH); 1606 (w), v(N=C); 654 (s), v(SbF$_6$). ^{1}H NMR (500.10

MHz, CD$_2$Cl$_2$, RT): δ = 8.40 (bs, 1H, NH $trans$ Os), 8.17 (s, 1H, NH $trans$ CH$_2$), 7.79

- 7.25 (m, 10H, PPh$_2$), 6.97 - 6.00 (m, 8H, Ar), 6.56 (d, J(H$_A$,H$_B$) = 5.8 Hz, 1H, H$_B$),

5.88 (d, 1H, H$_A$), 5.84 (d, J(H$_{B'}$,H$_{A'}$) = 5.31 Hz, 1H, H$_{A'}$), 5.49 (bs, 1H, H$_{B'}$), 3.90 (bm,

1H, H$_{pro-R}$ NCH$_2$), 3.23 (m, 1H, H$_{pro-S}$ NCH$_2$), 2.99 (m, 1H, H$_{pro-R}$ PCH$_2$), 2.63 (m, 1H,

H$_{pro-S}$ PCH$_2$), 2.34 (m, 1H, CH iPr), 2.17, 2.15 (2 × s, 6H, Me p-Tol), 1.81 (s, 3H, Me

p-cymene), 1.20, 1.06 (2 × d, J(H,H) = 6.9 Hz, 6H, Me iPr). ^{13}C{^{1}H} NMR (125.77

MHz, CD$_2$Cl$_2$, RT): δ = 139.46-123.64 (Ar), 95.11 (C−iPr p-cymene), 83.21, 83.17

(CH$_A$, CH$_B$), 80.32 (CH$_{B'}$), 78.03 (CH$_{A'}$), 54.19 (CH$_2$N), 31.48 (CH iPr), 25.35 (d,

J(P,C) = 32.5, CH$_2$P), 23.84, 22.90 (Me iPr), 21.36 (2 × Me, p-Tol), 18.25 (Me p-

cymene). $^{31}P\{^1H\}$ NMR (202.46 MHz, CD_2Cl_2, RT): δ = 22.69 (bs). ^1H NMR (500.10 MHz, CD_2Cl_2, 193 K): Major isomer: δ = 9.97, 8.26 (2 × s, 2H, NH), 7.80 - 7.27 (m, 10H, PPh_2), 7.27 - 6.21 (m, 8H, Ar), 6.60, 6.01 (2 × d, $J(H_A,H_B)$ = 5.5 Hz, 2H, H_A, H_B), 5.66, 5.32 (2 × d, $J(H_{B'},H_{A'})$ = 5.5 Hz, 2H, $H_{A'}$, $H_{B'}$), 4.18 (m, 1H, H_{pro-R} NCH_2), 3.26 (m, 1H, H_{pro-S} NCH_2), 3.00, 2.53 (2 × m, 2H, PCH_2), 2.08, 2.01 (2 × s, 6H, Me p-Tol), 1.95 (m, 1H, CH iPr), 1.56 (s, 3H, Me p-cymene), 1.07bs, 0.95 (d, $J(H,H)$ = 5.6 Hz) (6H, Me iPr). Minor isomer: δ = 8.65, 8.23 (2 × s, 2H, NH), 6.50, 5.90 (2 × d, $J(H_A,H_B)$ = 6.0 Hz, 2H, H_A H_B), 5.74, 5.58 (2 × d, $J(H_{B'},H_{A'})$ = 5.4 Hz, 2H, $H_{A'}$ $H_{B'}$), 3.08 (m, 1H, H_{pro-R} NCH_2), 2.81 (m, 1H, H_{pro-S} NCH_2), 2.81, 2.45 (2 × m, 2H, PCH_2), 2.40 (m, 1H, CH iPr), 2.31, 2.22 (2 × s, 6H, Me p-Tol), 1.80 (s, 3H, Me p-cymene), 1.08, 1.03 (2 × bs, 6H, Me iPr). $^{13}C\{^1H\}$ NMR (125.77 MHz, CD_2Cl_2, 193 K): Major isomer: δ = 153.00 (C=N), 139.90-122.11 (Ar), 102.16, 95.79 (C−Me, C−iPr, p-cymene), 83.09, 82.16 (CH_A, CH_B), 79.26, 74.94 ($CH_{B'}$, $CH_{A'}$), 54.24 (CH_2N), 23.02 (CH_2P), 30.44 (CH, iPr), 23.58, 21.86 (Me, iPr), 20.77, 20.74 (2 × Me, p-Tol), 17.45 (Me, p-cymene). Minor isomer: δ = 156.71 (C=N), 139.90-122.11 (Ar), 104.39, 93.58 (C−Me, C−iPr, p-cymene), 81.34, 80.84 (CH_A, CH_B), 79.48, 76.94 ($CH_{B'}$, $CH_{A'}$), 55.22, 23.86 (CH_2N, CH_2P), 23.58, 21.74 (Me, iPr), 21.10, 21.03 (2 × Me, p-Tol), 17.85 (Me, p-cymene). $^{31}P\{^1H\}$ NMR (202.46 MHz, CD_2Cl_2, 193 K): Major isomer: δ = 22.62 (s). Minor isomer: 25.52 (s).

Preparation of the complexes [(η^6-p-cymene)Os(H₂L1)(L)][SbF₆]₂ (L = Py (6), 4-NHMePy (7)

To a solution of the complex [(η^6-p-cymene)Os(**H₂L1**)(OH₂)][SbF₆]₂ (**4**) (185.2 mg, 0.20 mmol) in CH_2Cl_2 (10 mL), 0.20 mmol of the corresponding pyridine was added. The resulting solution was stirred for 5 h and concentrated under reduced pressure to

ca. 2 mL. The slow addition of hexane led the precipitation of a yellow (py) or brown (4-NHMepy) solid, which was washed with hexane (3 × 5 mL) and vacuum-dried. Crystals of **6** suitable for X-ray diffraction analysis were obtained by crystallisation from CH_2Cl_2.

6
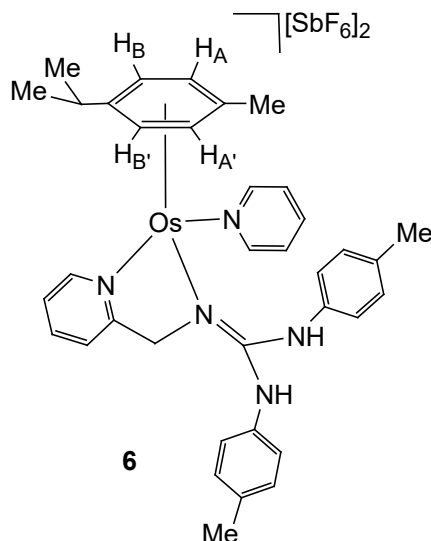
Complex 6. Yield: 195.3 mg, 81 %. Anal. Calcd for $C_{36}H_{41}N_5F_{12}OsSb_2$: C, 35.9; H, 3.4; N, 5.8. Found: C, 35.7; H, 3.2; N, 5.9. HRMS (*μ*-TOF), $C_{36}H_{41}N_5F_{12}OsSb_2$, [M−2SbF$_6$−Py−H]$^+$, calcd: 655.2472, found: 655.2479. IR (cm^{-1}): 3378 (br), v(NH); 1606 (m), v(N=C); 651 (s), v(SbF$_6$). ^{1}H NMR (500.10 MHz, CD$_2$Cl$_2$, RT): δ = 9.09 (bd, J(H$_5$Py,H$_6$Py) = 7.2 Hz, 1H, H$_6$ Py κ^2*N,N'* ligand), 8.57 (bd, J(H$_3$Py,H$_2$Py) = J(H$_5$Py,H$_6$Py) = 7.1 Hz, 2H, H$_2$ H$_6$ Py), 7.97 (t, J(H$_3$Py,H$_4$Py) ≈ J(H$_5$Py,H$_4$Py) = 7.1 Hz, 1H, H$_4$ Py), 7.88 (t, J(H$_3$Py,H$_4$Py) ≈ J(H$_5$Py,H$_4$Py) = 7.3 Hz, 1H, H$_4$ Py κ^2*N,N'* ligand), 7.59 (t, J(H$_2$Py,H$_3$Py) ≈ J(H$_4$Py,H$_3$Py) ≈ J(H$_4$Py,H$_5$Py) ≈ J(H$_6$Py,H$_5$Py) = 7.1 Hz, 2H, H$_3$ H$_5$ Py), 7.48 (t, J(H$_4$Py,H$_5$Py) ≈ J(H$_6$Py,H$_5$Py) = 7.2 Hz, 1H, H$_5$ Py κ^2*N,N'* ligand), 7.39 (bd, J(H$_4$Py,H$_3$Py) = 7.3 Hz, 1H, H$_3$ Py κ^2*N,N'* ligand), 7.15 (s, 2H, NH), 7.04, 6.97 (AB system, J(A,B) = 7.7 Hz, 8H, Ar), 6.25 (d, J(H$_A$,H$_B$) = 5.8 Hz, 1H, H$_B$), 6.22 (d, J(H$_A'$,H$_B'$) = 5.8 Hz, 1H, H$_B'$), 6.12 (d, 1H, H$_A$), 6.01 (d, 1H, H$_A'$), 5.04 (A part of an AB system, J(H$_{pro-R}$,H$_{pro-S}$) = 18.9 Hz, 1H, CH*H$_{pro-S}$*), 4.88 (B part of an

AB system, 1H, CH*H*$_{pro-R}$), 2.47 (spt, 1H, CH *i*Pr), 2.22 (s, 6H, Me *p*-Tol), 2.00 (s, 3H, Me *p*-cymene), 1.05 (d, *J*(H,H) = 6.7 Hz, 6H, Me *i*Pr). ^{13}C{^{1}H} NMR (125.77 MHz, CD$_2$Cl$_2$, RT): δ = 162.90 (C$_2$ Py κ^2*N,N'* ligand), 157.36 (C=N), 154.20 (C$_6$ Py κ^2*N,N'* ligand), 153.79 (C$_2$, C$_6$ Py), 141.60 (C$_4$ Py κ^2*N,N'* ligand), 141.45 (C$_4$ Py), 136.62, 134.92, 131.06 (Ar), 129.05 (C$_3$, C$_5$ Py), 127.90 (C$_5$ Py κ^2*N,N'* ligand), 122.59 (C$_3$ Py κ^2*N,N'* ligand), 122.10 (Ar), 97.24 (*C*−Me *p*-cymene), 97.07 (*C*−*i*Pr *p*-cymene), 81.35 (CH$_B$), 80.26 (CH$_{B'}$), 75.71 (CH$_A$), 75.80 (CH$_{A'}$), 61.56 (CH$_2$), 32.31 (CH *i*Pr), 23.31, 23.11 (Me *i*Pr), 21.28 (2 × Me *p*-Tol), 18.23 (Me *p*-cymene).
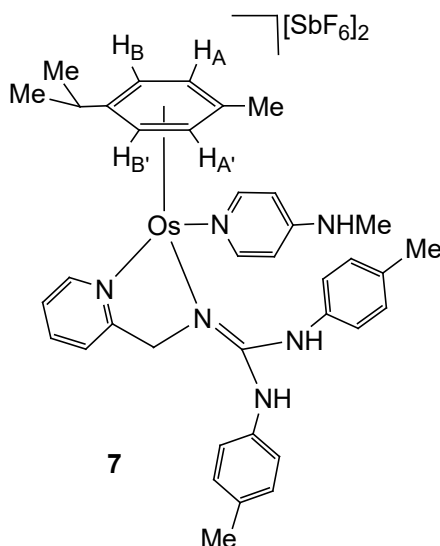

Complex 7. Yield: 212.6 mg, 84 %. Anal. Calcd. for C$_{37}$H$_{44}$N$_6$F$_{12}$OsSb$_2$: C, 36.0; H, 3.6; N, 6.8. Found: C, 35.8; H, 3.3; N, 6.9. HRMS (*μ*-TOF), C$_{37}$H$_{44}$N$_6$F$_{12}$OsSb$_2$, [M−2SbF$_6$−4-NHMepy−H]$^+$, calcd: 655.2472, found: 655.2455. IR (cm^{-1}): 3380 (br), *v*(NH); 1625 (m), 1608 (m), *v*(N=C); 652 (s), *v*(SbF$_6$). ^{1}H NMR (300.13 MHz MHz, CD$_2$Cl$_2$, RT): δ = 8.91 (bd, *J*(H$_5$Py,H$_6$Py) = 7.3, 1H, H$_6$ Py κ^2*N,N'* ligand), 7.88 (t, *J*(H$_3$Py,H$_4$Py) ≈ *J*(H$_5$Py,H$_4$Py) = 7.4 Hz, 1H, H$_4$ Py κ^2*N,N'* ligand), 7.85 (m, 2H, H$_2$ H$_6$ Py), 7.48 (bd, *J*(H$_4$Py,H$_3$Py) = 7.4 Hz, 1H, H$_3$ Py κ^2*N,N'* ligand), 7.42 (t, *J*(H$_6$Py,H$_5$Py) = 7.3 Hz, 1H, H$_5$ Py κ^2*N,N'* ligand), 7.01, 6.91 (AB system, *J*(A,B) = 8.3 Hz, 8H, Ar), 6.56 (d, 2H, *J*(H$_2$Py,H$_3$Py) ≈ *J*(H$_6$Py,H$_5$Py) = 7.0 Hz, H$_3$ H$_5$ Py), 6.12,

6.10, 6.05, 5.96 (4 × d, J(H_A,H_B) ≈ J($H_{A'}$,$H_{B'}$) = 6.2 Hz, 4H, H_A $H_{A'}$ H_B $H_{B'}$), 5.37 (q, 1H, N*H*Me), 5.23 (A part of an AB system, J(H_{pro-S},H_{pro-R}) = 18.7 Hz, 1H, CH*H*$_{pro-R}$), 5.06 (B part of an AB system, 1H, CH*H*$_{pro-S}$), 2.88 (d, J(H,H) = 5.1 Hz, 3H, NH*Me*), 2.41 (spt, 1H, CH *i*Pr), 2.20 (s, 6H, Me *p*-Tol), 2.05 (s, 3H, Me *p*-cymene), 1.06, 1.00 (2 × d, J(H,H) = 6.7, 6H, Me *i*Pr). ^{13}C{^{1}H} NMR (100.62 MHz, CD_2Cl_2, RT): δ = 162.46 (C_2 Py κ^2*N,N'* ligand), 156.63 (C_4 Py), 156.01 (C=N), 154.16 (C_6 Py κ^2*N,N'* ligand), 141.26 (C_5 Py κ^2*N,N'* ligand), 136.16, 135.11, 130.88, (Ar), 127.53 (C_4 Py κ^2*N,N'* ligand), 122.49 (C_3 Py κ^2*N,N'* ligand), 121.88 (Ar), 98.36, 93.80 (*C*−Me *p*-cymene, *C*−*i*Pr), 79.26. 79.22, 78.10, 76.94 (CH$_A$ CH$_B$ CH$_{A'}$ CH$_{B'}$), 61.80 (CH$_2$), 32.12 (CH *i*Pr), 30.05 (NHMe) 23.78, 22.47 (Me *i*Pr), 21.26 (2 × Me *p*-Tol), (Me *p*-cymene).

Preparation of the complex [(η^6-*p*-cymene)Os(H₂L1)(CO)][SbF₆]₂ (8)

After bubbling of carbon monoxide through a dichloromethane/acetone solution (7 ml, 2.5/1, V/V) of the complex [(η^6-*p*-cymene)Os(**H₂L1**)(OH₂)][SbF₆]₂ (**4**) (228.9 mg, 0.2 mmol) for 30 min, the slow addition of hexane led to the precipitation of a yellow solid which was washed with hexane (3 × 10 mL) and vacuum-dried. Crystals of **8** suitable for X-ray diffraction analysis were obtained by crystallisation from CH_2Cl_2.

8
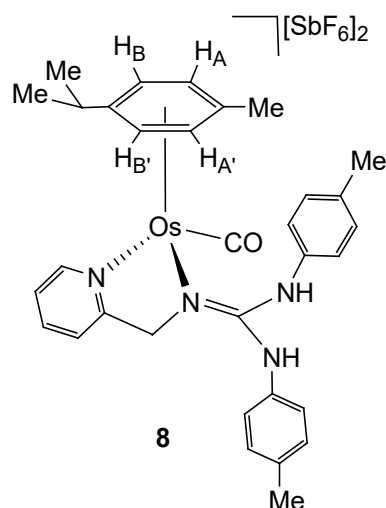
Complex 8. Yield: 203.2 mg, 88 %. Anal. Calcd for $C_{32}H_{36}N_4F_{12}OOsSb_2$: C, 33.3; H, 3.1; N, 4.8. Found: C, 33.0; H, 3.0; N, 4.7. HRMS (μ-TOF), $C_{32}H_{36}N_4F_{12}OOsSb_2$, $[M-2SbF_6-H]^+$, calcd: 683.2421, found: 683.2432. IR (cm^{-1}): 3379 (br), ν(NH); 2024 (m), ν(CO); 1607 (m), ν(N=C); 652 (s), ν(SbF$_6$). ^{1}H NMR (300.13 MHz, CD$_2$Cl$_2$, RT): δ = 8.86, (bd, J(H$_5$Py,H$_6$Py) = 7.1 Hz, 1H, H$_6$ Py), 8.10 (t, J(H$_3$Py,H$_4$Py) ≈ J(H$_5$Py,H$_4$Py) = 7.2 Hz, 1H, H$_4$ Py), 7.65 (bd, J(H$_4$Py,H$_3$Py) = 7.2, 1H, H$_3$ Py), 7.56 (t, J(H$_4$Py,H$_5$Py) ≈ J(H$_6$Py,H$_5$Py) = 7.1 Hz, 1H, H$_5$ Py), 7.55 (s, 1H, NH *trans* CH$_2$), 6.98 (bs), 6.91(d) (AB system, J(A,B) = 8.2 Hz, 8H, Ar), 6.67, 6.55 (m, 4H, H$_A$ H$_B$, H$_{A'}$ H$_{B'}$), 6.07 (s, 1H, NH *trans* Os), 5.58 (A part of an AB system, J(H$_{pro\text{-}S}$,H$_{pro\text{-}R}$) = 18.7 Hz, 2H, CH$H_{pro\text{-}R}$), 5.16 (B part of an AB system, 2H, CH$H_{pro\text{-}S}$), 2.48 (spt, 1H, CH *i*Pr), 2.20, 2.18, 2.12 (3 × s, 9H, Me *p*-Tol, Me *p*-cymene), 1.20, 1.12 (2 × d, J(H,H) = 6.9 Hz, 6H, Me *i*Pr). ^{13}C{^{1}H} NMR (100.62 MHz, (CD$_3$)$_2$CO, RT): δ = 174.81 (CO), 163.34 (C$_2$ Py), 160.52 (C=N), 158.08 (C$_6$ Py), 143.39 (C$_4$ Py), 137.09, 136.59, 131.40 (Ar), 128.11 (C$_5$ Py), 124.02 (C$_3$ Py), 123.89 (Ar), 120.52, 118.86 (*C*−Me *p*-cymene, *C*−*i*Pr), 94.75, 91.28, 91.13, 90.82 (CH$_A$ CH$_B$ CH$_{A'}$ CH$_{B'}$), 65.52 (CH$_2$), 33.46 (CH *i*Pr), 23.74, 23.27 (Me *i*Pr), 21.49 (2 × Me *p*-Tol) 19.99 (Me *p*-cymene).

Preparation of the complex [(η^6-p-cymene)Os(H₂L1)(P(OMe)₃)][SbF₆]₂ (9)

To a solution of the complex [(η^6-*p*-cymene)Os*(H₂L1)*(OH₂)][SbF₆]₂ (**4**) (185.2 mg, 0.20 mmol) in dichloromethane (10 mL), 23.6 μL (0.20 mmol) of P(OMe)₃ were added. The resulting solution was stirred for 24 h and concentrated under reduced pressure to *ca*. 2 mL. The slow addition of hexane led the precipitation of a brown solid, which were washed with hexane (3 × 5 mL) and vacuum-dried.
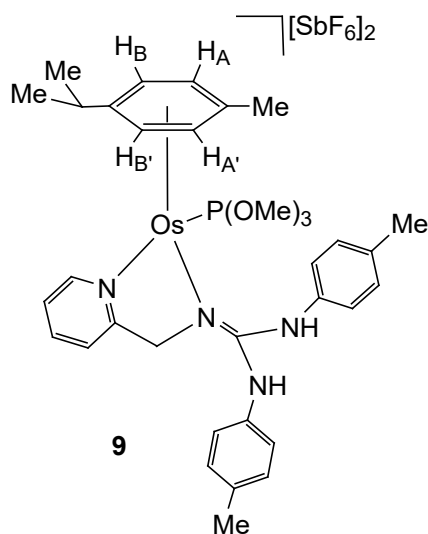

Complex 9. Yield: 217.6 mg, 87 %. Anal. Calcd for $C_{34}H_{45}N_4F_{12}O_3OsPSb_2$: C, 32.7; H, 3.6; N, 4.5. Found: C, 32.7; H, 3.3; N, 4.6. HRMS (*μ*-TOF), $C_{34}H_{45}N_4F_{12}O_3OsPSb_2$, [M−2SbF₆−H]⁺, calcd: 655.2472, found: 655.2459. IR (cm⁻¹): 3341 (br), *v*(NH); 1022 (m), *v*(PO); 1611 (m), *v*(N=C); 651 (s), *v*(SbF₆). ¹H NMR (500.10 MHz, CD₂Cl₂, RT): δ = 8.83 (bd, $J(H_5Py,H_6Py)$ = 8.0 Hz, 1H, H₆ Py), 8.01 (t, $J(H_3Py,H_4Py) \approx J(H_5Py,H_4Py)$ = 7.9 Hz, 1H, H₄ Py), 7.54 (bd, $J(H_4Py,H_3Py)$ = 7.9 Hz, 1H, H₃ Py), 7.53 (t, $J(H_4Py,H_5Py) \approx J(H_6Py,H_5Py)$ = 8.0 Hz, 1H, H₅ Py), 7.39 (s, 1H, NH *trans* Os), 7.27 (s, 1H, NH *trans* CH₂), 7.02, 6.83 (AB system, $J(A,B)$ = 8.3 Hz, 4 H, Ar), 6.95, 6.86 (AB system, $J(A,B)$ = 8.3 Hz, 4 H, Ar), 6.29 (d, $J(H_{A'},H_{B'})$ = 5.8 Hz, 1H, H_{B'}), 6.20 (d, $J(H_A,H_B)$ = 5.7 Hz, 1H, H_A), 6.03 (d, 1H, H_B), 5.98 (d, 1H, H_{A'}), 5.45 (A part of an AB system, $J(H_{pro-S},H_{pro-R})$ = 18.7 Hz, 1H, CH*H_{pro-R}*), 5.15 (B part

of an AB system, 1H, CHH_{pro-S}), 3.81 (d, J(PH) = 11.1 Hz, 9H, OMe), 2.32 (spt, 1H, CH iPr), 2.20, 2.18 (s, 6H, Me p-Tol), 2.12 (s, 3H, Me p-cymene), 1.17, 0.80 (2 × d, J(H,H) = 7.0 Hz, 6H, Me iPr). ^{13}C{^{1}H} NMR (125.77 MHz, CD$_2$Cl$_2$, RT): δ = 164.02 (C$_2$ Py), 156.78 (C$_6$ Py), 156.76 (C=N), 141.58 (C$_4$ Py), 135.71, 135.50, 135.41, 135.05, 131.16, 130.43 (Ar), 127.62 (C$_5$ Py), 122.16 (C$_3$ Py), 121.64 (d, J(P,C) = 7.5 Hz, C−Me p-cymene), 121.32, 120.76 (Ar), 97.85 (C−iPr p-cymene), 87.76 (CH$_A$), 86.40 (CH$_{A'}$), 85.15 (d, J(P,C) = 11.9 Hz, CH$_{B'}$), 77.43 (CH$_{A'}$), 63.39 (CH$_2$), 56.22 (d, J(P,C) = 9.2 Hz, OMe), 32.04 (CH iPr), 23.95, 19.92 (Me iPr), 21.22, 21.20 (2 × Me p-Tol), 12.9 (Me p-cymene). ^{31}P{^{1}H} NMR (202.46 MHz, CD$_2$Cl$_2$, RT, ppm): δ = 74.32 (s).

Preparation of the complexes [(η^6-p-cymene)Os(κ^3N,N',N''-HL1)][SbF$_6$] (10) and [(η^6-p-cymene)Os(κ^3N,N',P-HL2)][SbF$_6$] (11)

To a solution of the corresponding complex [(η^6-p-cymene)Os(**H$_2$L**) (OH$_2$)][SbF$_6$]$_2$ (**H$_2$L** = **H$_2$L1 (4)**, **H$_2$L2 (5)**) (0.2 mmol)) in methanol (20 mL), 16.8 mg (0.2 mmol) of solid NaHCO$_3$ were added. The resulting suspension was stirred for 15 h and then was vacuum-evaporated to dryness. The residue was extracted with dichloromethane and the resulting solution was concentrated under reduced pressure to $ca.$ 2 mL. The slow addition of hexane led to the precipitation of a yellow solid, which was washed with hexane (3 × 10 mL) and vacuum-dried. Crystals of **11** suitable for X-ray diffraction analysis were obtained by crystallisation from CH$_2$Cl$_2$/hexane solutions.
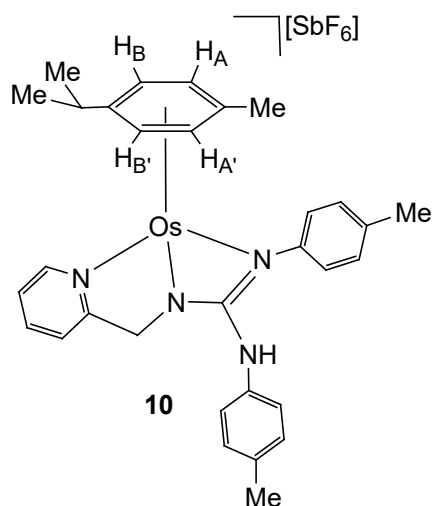
Complex 10. Yield: 148.8 mg, 85 %. Anal. Calcd for $C_{31}H_{35}N_4F_6OsSb$: C, 41.85; H, 4.0; N, 6.3. Found: C, 42.1; H, 4.0; N, 6.0. HRMS (μ-TOF), $C_{31}H_{35}N_4F_6OsSb$, [M−SbF$_6$]$^+$, calcd: 655.2472, found: 655.2495. IR (cm^{-1}): 3359 (br), v(NH); 1628 (m), v(N=C); 654 (s), v(SbF$_6$). ^{1}H NMR (500.10 MHz, CD$_2$Cl$_2$, RT): δ = 9.27, (bd, J(H$_5$Py,H$_6$Py) = 7.2 Hz, 1H, H$_6$ Py), 7.81 (t, J(H$_3$Py,H$_4$Py) ≈ J(H$_5$Py,H$_4$Py) = 7.3 Hz, 1H, H$_4$ Py), 7.41 (t, J(H$_4$Py,H$_5$Py) ≈ J(H$_6$Py,H$_5$Py) = 7.2 Hz, 1H, H$_5$ Py), 7.30 (bd, J(H$_4$Py,H$_3$Py) = 7.3 Hz, 1H, H$_3$ Py), 7.13, 6.92 (AB system, J(A,B) = 8.4 Hz, 4 H, Ar), 7.13, 6.98 (AB system, J(A,B) = 8.4 Hz, 4 H, Ar), 6.15 (s, 1H, NH), 5.89, 5.88 (2 × d, J(H$_A$,H$_B$) = J(H$_{A'}$,H$_{B'}$) = 5.1, 2H, H$_B$ H$_{B'}$), 5.73, 5.71 (2 × d, 2H, H$_A$ H$_{A'}$), 5.35 (A part of an AB system, J(H$_{pro-S}$,H$_{pro-R}$) = 17.2, 1H, CHH_{pro-R}), 4.13 (B part of an AB system, 1H, CHH_{pro-S}), 2.42 (spt, 1H, CH iPr), 2.31, 2.30 (s, 6H, Me p-Tol), 2.09 (s, 3H, Me p-cymene), 1.17, 1.14 (2 × d, J(HH) = 7.0 Hz, 6H, Me iPr). ^{13}C{^{1}H} NMR (125.77 MHz, CD$_2$Cl$_2$, RT): δ = 169.61 (C=N), 164.85 (C$_2$ Py), 155.50 (C$_6$ Py), 140.35 (C$_4$ Py), 136.28, 135.49, 134.63, 131.13, 130.98 (Ar), 125.93 (C$_5$ Py), 123.42 (Ar), 122.54 (C$_3$ Py), 120.26 (Ar), 93.42 (*C*−Me p-cymene), 90.23 (*C*−iPr), 74.77 (CH$_B$ CH$_{B'}$), 73.58, 73.49 (CH$_A$ CH$_{A'}$), 59.35 (CH$_2$), 32.47 (CH iPr), 23.58, 23.00 (Me iPr), 21.40, 21.31 (2 × Me p-Tol), 19.35 (Me p-cymene).

11
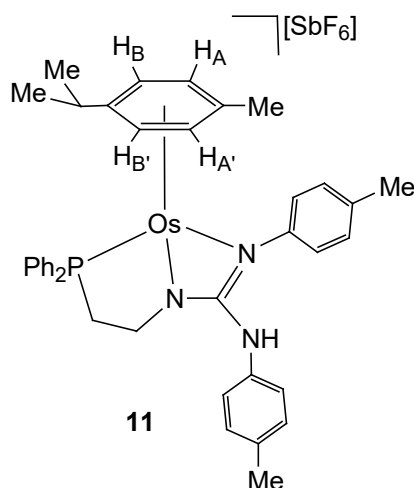
Complex 11. Yield: 192.0 mg, 95 %. Anal. Calcd for C$_{39}$H$_{43}$N$_3$F$_6$POsSb·1/2CH$_2$Cl$_2$: C, 45.0; H, 4.2; N, 4.0. Found: C, 44.9; H, 4.0; N, 4.0. HRMS (μ-TOF), C$_{39}$H$_{43}$N$_3$F$_6$POsSb, [M−SbF$_6$]$^+$, calcd: 776.2806, found: 776.2839. IR (cm^{-1}): 3341 (w), ν(NH); 1593 (w), ν(N=C); 654 (s), ν(SbF$_6$). ^{1}H NMR (500.10 MHz, CD$_2$Cl$_2$, RT): δ= 7.76 - 7.23 (m, 10H, PPh$_2$), 7.02, 6.67 (2 × bs, 4 H, Ar), 6.99, 6.74 (AB system, J(A,B) = 7.8 Hz, 4 H, Ar), 5.76 (s, 1H, NH), 5.40, 5.35, 4.80 (3 × bs, 4H, H$_A$ H$_B$ H$_{A'}$ H$_{B'}$), 3.40 (bm, 1H, NCHH_{pro-R}), 2.98 (bm, 1H, NCHH_{pro-S}), 2.68 (bm, 1H, CH iPr), 2.54 (m, 1H, PCHH_{pro-S}), 2.52 (m, 1H, PCHH_{pro-R}), 2.27 (s, 6H, Me p-Tol), 2.25 (s, 3H, Me p-cymene), 1.29 (bd, J(HH) = 7.0 Hz, 3H, Me iPr). ^{13}C{^{1}H} NMR (125.77 MHz, CD$_2$Cl$_2$, RT): δ = 135.60-123.14 (Ar), 52.16 (CH$_2$N), 34.45 (d, J(P,C) = 32.52, CH$_2$P), 32.63 (CH iPr), 24.17, 22.67 (Me iPr), 21.32, 21.21 (2 × Me p-Tol), 19.40 (Me p-cymene). ^{31}P{^{1}H} NMR (202.46 MHz, CD$_2$Cl$_2$, RT): δ = 23.87 (bs).

General procedure for the catalytic reaction of *N*-methyl-2-methylindole with *trans-β*-nitrostyrene

Catalyst (0.03 mmol), *trans-β*-nitrostyrene (0.90 mmol) and dry CH$_2$Cl$_2$ (2 mL) were mixed under argon at room temperature in a Schlenk flask equipped with a magnetic

stirrer. The resulting mixture was stirred for 15 min and then *N*-methyl-2-methylindole (0.60 mmol) was added. The course of the reaction was monitored by regularly taking samples of *ca*. 50 μL which, after quenching by addition of Et_2O, were concentrated under vacuum until dryness. The residue was extracted with Et_2O (4 × 3 mL) and the solution vacuum-evaporated until dryness, dissolved in $CDCl_3$ and analysed by ^1H NMR. Conversion values were determined by integration of the ^1H NMR signals of the C3-H proton of the *N*-methyl-2-methylindole (*ca*. 6.1 ppm) and that of the $CHCH_2NO_2$ protons of the adduct (*ca*. 5.1 ppm). The collected results are the average of at least two comparable reaction runs.

X-ray crystallography

X-ray diffraction data were collected on a Smart APEX (compound **1**, **3**, **4**, **6**, **8** and **11**) or APEX DUO (complex **2**) Bruker diffractometers, using graphite-monochromated Mo κα radiation (λ = 0.71073 Å). Single crystals were mounted on a fiber, coated with a protecting perfluoropolyether oil and cooled to 100(2) K or 120(2) K (in the case of compound **11**) with an open-flow nitrogen gas. Data were collected using ω-scans with narrow oscillation frame strategy (Δω = 0.3°). Diffracted intensities were integrated and corrected of absorption effects by using multi-scan method using SAINT[25] and SADABS[26] programs, included in APEX2 package. Structures were solved by direct methods with SHELXS[27] and refined by full-matrix least squares on F^2 with SHELXL program[28] included in Wingx program system.[29]

Hydrogen atoms have been observed in Fourier difference maps. Most of them have been included in the model in calculated positions and refined with a riding model. Those of NH fragments have been included in observed positions, with geometrical restraints concerning N−H bond lengths.

Large solvent accessible voids are observed in the unit cell of compounds **1** and **11**. However, the solvent is highly disordered and no attempt to include it in the model lead to adequate results. Therefore, Squeeze corrections[30] have been applied. The total potential accessible void volume and the electron count agree with the presence of three methanol molecules and four dichloromethane molecules in the unit cell of compound **1** and **11**, respectively. They have been taken into account in the chemical formula, F000 and density.

Compound **6** has been refined as a 2-component twin related by a 180 degres rotation around reciprocal *b* axis. Unit cell and domain orientation matrices were determined with Cell Now program.[31] Absorption corrections were performed with Twinabs program.[32] Final structural model refinement leads to a 0.289 BASF value.

Crystal structure determination for complex 1. $C_{31}H_{36}ClF_6N_4OsSb \cdot 1.5(CH_4O)$; M_r = 974.10; yellow plate, $0.050 \times 0.070 \times 0.200$ mm^3; triclinic $P\bar{1}$; a = 10.8413(6) Å, b = 11.1473(6) Å, c = 15.2059(6) Å, α = 92.1850(10)°, β = 93.7980(10)°, γ = 110.5430(10)°; V = 1713.31(15) Å^3, Z = 2, D_c = 1.888 g/cm^3; μ = 4.638 cm^{-1}; min. and max. absorption correction factors: 0.5093 and 0.6974; $2\theta_{max}$ = 57.24°; 21006 reflections measured, 7990 unique; R_{int} = 0.0313; number of data/restraint/parameters 7990/2/410; R_1 = 0.0287 [7033 reflections, $I > 2\sigma(I)$], w$R(F^2)$ = 0.0633 (all data); largest difference peak 1.322 e.Å^{-3}.

Crystal structure determination for complex 2. $C_{39}H_{44}ClF_6N_3OsPSb$; M_r = 1047.14; yellow prism, $0.146 \times 0.255 \times 0.293$ mm^3; orthorhombic $P2_12_12_1$; a = 10.9424(4) Å, b = 13.4216(5) Å, c = 25.9506(10) Å, V = 3811.2(2) Å^3, Z = 4, D_c = 1.825 g/cm^3; μ = 4.214 cm^{-1}; min. and max. absorption correction factors: 0.3736 and 0.5016; $2\theta_{max}$ = 59.55°; 95284 reflections measured, 10435 unique; R_{int} = 0.0331;

number of data/restraint/parameters 10435/1/498; $R_1 = 0.0175$ [10312 reflections, $I > 2\sigma(I)$], $wR(F^2) = 0.0411$ (all data); largest difference peak 1.255 e.Å^{-3}.

Crystal structure determination for complex 3.
$2(C_{39}H_{45}Cl_2F_6N_3OsPSb)\cdot2(CH_2Cl_2)\cdot3/2(C_6H_{14})$; $M_r = 2466.30$; orange prism, $0.160 \times 0.200 \times 0.224$ mm^3; triclinic $P\bar{1}$; $a = 11.0006(6)$ Å, $b = 17.8189(9)$ Å, $c = 26.0251(13)$ Å, $\alpha = 99.1650(10)°$, $\beta = 100.6070(10)°$, $\gamma = 97.5640(10)°$; $V = 4881.6(4)$ Å^3, $Z = 2$, $D_c = 1.678$ g/cm^3; $\mu = 3.463$ cm^{-1}; min. and max. absorption correction factors: 0.5077 and 0.6145; $2\theta_{max} = 56.81°$; 110689 reflections measured, 23468 unique; $R_{int} = 0.0432$; number of data/restraint/parameters 23468/7/1123; $R_1 = 0.0363$ [19137 reflections, $I > 2\sigma(I)$], $wR(F^2) = 0.0989$ (all data); largest difference peak 2.620 e.Å^{-3}.

Crystal structure determination for complex 4.
$C_{31}H_{38}F_{12}N_4OOsSb_2\cdot2(CH_2Cl_2)$; $M_r = 1314.20$; yellow prism, $0.110 \times 0.160 \times 0.165$ mm^3; triclinic $P\bar{1}$; $a = 8.709(8)$ Å, $b = 15.2562(14)$ Å, $c = 17.6428(16)$ Å, $\alpha = 110.1590(10)°$, $\beta = 92.3050(10)°$, $\gamma = 98.7480(10)°$; $V = 2164(2)$ Å^3, $Z = 2$; $D_c = 2.017$ g/cm^3; $\mu = 4.499$ cm^{-1}; min. and max. absorption correction factors: 0.4359 and 0.6240; $2\theta_{max} = 56.31°$; 22268 reflections measured, 9848 unique; $R_{int} = 0.0627$; number of data/restraint/parameters 9848/4/531; $R_1 = 0.0636$ [6988 reflections, $I > 2\sigma(I)$], $wR(F^2) = 0.1383$ (all data); largest difference peak 2.354 e.Å^{-3}. Four fluorine atoms of a counterion have been found to be disordered. They have been included in the model in two sets of positions with complementary occupancy factors (0.60/0.40(2)). Hydrogen atoms of coordinated water have not been observed in Fourier difference maps. HFIX 137 instruction has been used to calculated their possible positions. Afterwards, the "three hydrogen atoms" have been refined with a restrain in O−H bond lengths. Their obtained U_{iso} value have been used as criteria to select the two most suitable positions.

Crystal structure determination for complex 6. $C_{36}H_{41}F_{12}N_5OsSb_2$; M_r = 1205.44; yellow prism, $0.060 \times 0.095 \times 0.100$ mm^3; triclinic $P\bar{1}$; a = 11.5507(13) Å, b = 11.8469(13) Å, c = 15.5684(17) Å, α = 72.5690(10)°, β = 80.2290(10)°, γ = 82.140(2)°; V = 1994.7(4) Å^3, Z = 2, D_c = 2.007 g/cm^3; μ = 4.612 cm^{-1}; min. and max. absorption correction factors: 0.5482 and 0.7505; $2\theta_{max}$ = 56.576°; 19485 reflections measured, 13387 unique; R_{int} = 0.0774; number of data/restraint/parameters 13387/1/518; R_1 = 0.0608 [9481 reflections, $I > 2\sigma(I)$], w$R(F^2)$ = 0.1352 (all data); largest difference peak 1.590 e.Å^{-3}.

Crystal structure determination for complex 8. $C_{32}H_{36}F_{12}N_4OsSb_2 \cdot 1.75(CH_2Cl_2)$; M_r = 1302.97; yellow prism, $0.115 \times 0.200 \times 0.200$ mm^3; triclinic $P\bar{1}$; a = 16.9772(9) Å, b = 17.1277(9) Å, c = 17.5280(9) Å, α = 84.7380(10)°, β = 66.4340(10)°, γ = 67.5710(10)°; V = 4307.2(4) Å^3, Z = 4, D_c = 2.009 g/cm^3; μ = 4.491 cm^{-1}; min. and max. absorption correction factors: 0.4426 and 0.5750; $2\theta_{max}$ = 56.70°; 64380 reflections measured, 20155 unique; R_{int} = 0.0424; number of data/restraint/parameters 20155/8/1059; R_1 = 0.0690 [14839 reflections, $I > 2\sigma(I)$], w$R(F^2)$ = 0.2048 (all data); largest difference peak 8.616 e.Å^{-3}.

Crystal structure determination for complex 11. $C_{39}H_{43}F_6N_3OsPSb \cdot CH_2Cl_2$; M_r = 1095.61; yellow plate, $0.090 \times 0.325 \times 0.440$ mm^3; orthorhombic $Pna2_1$; a = 24.6016(11) Å, b = 10.2764(5) Å, c = 16.4397(8) Å; V = 4156.2(3) Å^3, Z = 4, D_c = 1.751 g/cm^3; μ = 3.931 cm^{-1}; min. and max. absorption correction factors: 0.3161 and 0.4546; $2\theta_{max}$ = 57.31°; 53101 reflections measured, 9956 unique; R_{int} = 0.0465; number of data/restraint/parameters 9956/2/469; R_1 = 0.0232 [9428 reflections, $I > 2\sigma(I)$], w$R(F^2)$ = 0.0572 (all data); largest difference peak 2.173 e.Å^{-3}.

Computational details

DFT geometry optimizations and thermochemical calculations were carried out with the Gaussian 09 program package,[33] using the B3LYP-D3 hybrid functional.[34] Geometry optimizations were performed in the gas phase with the LanL2TZ(f) effective core potential basis set for the osmium atoms, and the 6-311G(d,p) basis set for the remaining ones. All minima (no imaginary frequencies) and transition states (one imaginary frequency) were characterized by calculating the Hessian matrix. ZPE and gas-phase thermal corrections (entropy and enthalpy, 298.15 K, 1 atm) from these analyses were calculated. The nature of the transition states was confirmed by IRC calculations.

Conflicts of interest

The authors declare that they have no known competing financial interests or personal relationships that could have appeared to influence the work reported in this paper.

Acknowledgements

Notes and references

1   *(a)* X.-Y. Cui, C.-H. Tan, D. Leow, *Org. Biomol. Chem.*, 2019, **17**, 4689-4699. *(b)* J. Francos, V. Cadierno, *Dalton Trans.*, 2019, **48**, 9021-9036. *(c)* S. Dong, X. Feng, X. Liu, *Chem. Soc. Rev.*, 2018, **47**, 8525-8540. *(d)* W. Cao, X. Liu, X. Feng, *Chin. Chem. Lett.*, 2018, **29**, 1201-1208. *(e) Topics in Heterocyclic Chemistry; Guanidines as Reagents and Catalysts I and II*, ed. P. Selig, Springer, Switzerland, 2017, vol. 50, pp. 1-178; vol 51, pp. 1-203. *(f)* F. T. Edelmann, *Adv. Organomet. Chem.*, 2013, **1**, 55-374. *(g)* P. Selig, *Synthesis*, 2013, 703-718. *(h)* J. E. Taylor, S. D. Bull, J. M. J. Williams, *Chem. Soc. Rev.*, 2012, **41**, 2109-2121. *(i)* F. T. Edelmann, *Chem. Soc. Rev.*, 2012, **41**, 7657-7672. *(j)* Y. Sohtome, K. Nagasawa, *Chem. Commun.*, 2012, **48**, 7777-7789. *(k)* S. Collins, *Coord. Chem. Rev.,* 2011, **255**, 118-138. *(l)* X. Fu, C.-H. Tan, *Chem. Commun.*, 2011, **47**, 8210-8222. *(m)* M. Terada, *J. Synth. Org. Chem. Jpn.,* 2010, **68**, 1159-1168. *(n)* M. P. Coles, *Chem. Commun.*, 2009, 3659-3676. *(o)* D. Leow, C.-H. Tan, *Chem. Asian J.,* 2009, **4**, 488-507. *(p)* F. T. Edelmann, *Chem. Soc. Rev.,* 2009, **38**, 2253-2268.

2   *(a)* T. Chlupatý, A. Ruzicka, *Coord. Chem. Rev.*, 2016, **314**, 103-113. *(b) The Chemistry of Guanidine, Guanidinium, and Guanidinate Compounds, Aust. J. Chem.,* 2014, Vol. 67 Number 7. *(c)* F. T. Edelmann, *Adv. Organomet. Chem.,* 2013, **61**, 55-374. *(d)* A. A. Trifonov, *Coord. Chem. Rev.,* 2010, **254**, 1327-1347. *(e)* C. Jones, *Coord. Chem. Rev.,* 2010, **254**, 1273-1289. *(f)* M. P. Coles, *Chem. Commun.*, 2009, 3659-3676. *(g)* F. T. Edelmann, *Adv. Organomet. Chem.*, 2008, **57**, 183-352. *(h)* P. J. Bailey, S. Pace, *Coord. Chem. Rev.*, 2001, **214**, 91-141.

3   M. K. Kiesewetter, E. J. Shin, J. L. Hedrick and R. M. Waymouth, *Macromolecules*, 2010, **43**, 2093-2107 and references therein.

4   *(a)* R. G. S. Berlinck, S. Romminger, *Nat. Prod. Rep.*, 2016, **33**, 456-490 and references therein. *(b)* P. Blondeau, M. Segura, R. Pérez-Fernández, J. de Mendoza, *Chem. Soc. Rev.*, 2007, **36**, 198-210 and references therein.

5   *(a)* F. A. Cotton, G. M. Chiarella, N. S. Dalal, C. A. Murillo, Z. Wang, M. D. Young, *Inorg. Chem.*, 2010, **49**, 319-324. *(b)* F. A. Cotton, N. S. Dalal, P. Huang, C. A. Murillo, A. C. Stowe, X. Wang, *Inorg. Chem.,* 2003, **42**, 670-672. *(c)* R. Clérac, F. A. Cotton, L. M. Daniels, J. P. Donahue, C. A. Murillo, D. J. Timmons, *Inorg. Chem.,* 2000, **39**, 2581-2584.

6   S. D. Robinson, A. Sahajpal, J. Steed, *Inorg. Chim. Acta,* 2000, **303**, 265-270.

7   *(a)* S. A. Gámez-Rivera, J. Francos, J. Borge, V. Cadierno, *Eur. J. Inorg. Chem.,* 2017, 4138-4146. *(b)* J. Francos, P. J. González-Liste, L. Menéndez-Rodríguez, P. Crochet, V. Cadierno, J. Borge, A. Antiñolo, R. Fernández-Galán, F. Carrillo-Hermosilla, *Eur. J. Inorg. Chem.,* 2016, 393-402.

8   *(a)* K. Brak, E. N. Jacobsen, *Angew. Chem. Int. Ed.,* 2013, **52**, 534-561. *(b)* M. Rueping, A. Kuenkel, I. Atodiresei, *Chem. Soc. Rev.,* 2011, **40**, 4539-4549. *(c)* J. Yu, F. Shi, L.-Z. Gong, *Acc. Chem. Res.,* 2011, **44**, 1156-1171. *(d)* M. Rueping, B. J. Nachtsheim, W. Ieawsuwan, I. Atodiresei, *Angew. Chem. Int. Ed.,* 2011, **50**, 6706-6720. *(e)* N. Kumagai, M. Shibasaki, Angew. *Chem. Int. Ed.,* 2011, **50**, 4760-4772. *(f)* M Terada, *Synthesis,* 2010, 1929-1982. *(g)* M. Terada, Bull. *Chem. Soc. Jpn.,* 2010, **83**, 101-119. *(h)* J. N. Johnston, H. Muchalski, T. L. Troyer, *Angew. Chem. Int. Ed.,* 2010, **49**, 2290-2298. *(i)* G. W. Amarante, M. Benassi, H. M. S. Milagre, A. A. C. Braga, F. Maseras, M. N. Eberlin, F.

Coelho, *Chem. Eur. J.,* 2009, **15**, 12460-12469. *(j)* Z. Zhang, P. Schreiner, *Chem. Soc. Rev.,* 2009, **38**, 1187-1198. *(k)* A. Dondoni, A. Massi, *Angew. Chem. Int. Ed.,* 2008, **47**, 4638-4660. *(l)* M. Terada, M. *Chem. Commun.,* 2008, 4097-4112. *(m)* X. Yu, W. Wang, *Chem. Asian. J.,* 2008, **3**, 516-532. *(n)* H. Miyabe, Y. Takemoto, *Bull. Chem. Soc. Jpn.,* 2008, **81**, 785-795. *(o)* T. Akiyama, *Chem. Rev.,* 2007, **107**, 5744-5758. *(p)* A. G. Doyle, E. N. Jacobsen, *Chem. Rev.,* 2007, **107**, 5713-5743. *(q)* S. J. Connon, *Angew. Chem. Int. Ed.,* 2006, **45**, 3909-3912. *(r)* M. S. Taylor, E. N. Jacobsen, *Angew. Chem. Int. Ed.,* 2006, **45**, 1520-1543. *(s)* S. J. Connon, *Chem. Eur. J.,* 2006, **12**, 5418-5427. *(t)* T. Akiyama, J. Itoh, K. Fuchibe, *Adv. Synth. Catal.,* 2006, **348**, 999-1010. *(u)* Y. Takemoto, *Org. Biomol. Chem.,* 2005, **3**, 4299-4306. *(v)* J. Seayad, B. List, *Org. Biomol. Chem.,* 2005, **3**, 719-724. *(w)* P. M. Pihko, Angew. *Chem. Int. Ed.,* 2004, **43**, 2062-2064. *(x)* P. R. Schreiner, *Chem. Soc. Rev.,* 2003, **32**, 289-296.

9   H. Yamamoto, K. Futatsugi, *Angew. Chem. Int. Ed.,* 2005, **44**, 1924-1942.

10   L. Zhang, E. Meggers, *Chem. Asian J.,* 2017, **12**, 2335-2342 and references therein.

11   A. Ehnbom, S. K. Ghosh, K. G. Lewis, J. A. Gladysz, *Chem. Soc. Rev.,* 2016, **45**, 6799-6811 and references therein.

12   A. Scherer, T. Mukherjee, F. Hampel, J. A. Gladysz, *Organometallics,* 2014, **33**, 6709-6722.

13   C. Thomas, J. A. Gladysz, *ACS Catal.,* 2014, **4**, 1134-1138.

14   T. Mukherjee, C. Ganzmann, N. Bhuvanesh, J. A. Gladysz, *Organometallics,* 2014, **33**, 6723-6737.

15   *(a)* C. M. McGuirk, M. J. Katz, C. L. Stern, A. A. Sarjeant, J. T. Hupp, O. K. Farha, C. A. Mirkin, *J. Am. Chem. Soc.,* 2015, **137**, 919-925. *(b)* C. M. McGuirk, C. L. Stern, C. A. Mirkin, *J. Am. Chem. Soc.,* 2014, **136**, 4689-4696. *(c)* C. M. McGuirk, J. Méndez-Arroyo, A. M. Lifschitz, C. A. Mirkin, *J. Am. Chem. Soc.* 2014, **136**, 16594-16601.

16   D. Carmona, M. P. Lamata, A. Sánchez, F. Viguri, R. Rodríguez, L. A. Oro, C. Liu, S. Díez-González, F. Maseras, *Dalton Trans.,* 2014, **43**, 11260-11268.

17   D. Carmona, M. P. Lamata, A. Sánchez, P. Pardo, R. Rodríguez, P. Ramírez, F. J. Lahoz, P. García-Orduña, L. A. Oro, *Organometallics,* 2014, **33**, 4016-4026.

18   D. Carmona, M. P. Lamata, P. Pardo, R. Rodríguez, F. J. Lahoz, P. García-Orduña, I. Alkorta, J. Elguero, L. A. Oro, *Organometallics,* 2014, **33**, 616-619.

19   See for example: Á. Ávila, R. Chinchilla, E. Gómez-Bengoa, C. Nájera, *Eur. J. Org. Chem.,* 2013, 5085-5092.

20   J. Cabeza, P. M. Maitlis, *J. Chem. Soc., Dalton Trans.,* 1985, 573-578.

21   *(a)* R. S. Cahn, C. Ingold, V. Prelog, Angew. *Chem., Int. Ed. Engl.,* 1966, **5**, 385-415. *(b)* V. Prelog, G. Helmchen, *Angew. Chem., Int. Ed. Engl.,* 1982, **21**, 567-583. *(c)* C. Lecomte, Y. Dusausoy, J. Protas, J. Tirouflet, A. Dormond, *J. Organomet. Chem.,* 1974, **73**, 67-76.

22   F. H. Allen, O. Kennard, D. G. Watson, L. Brammer, A. G. Orpen, R. Taylor *J. Chem. Soc., Perkin Trans. 2*, 1987, S1-S19.

23   *(a) Dynamic NMR Spectroscopy,* ed. J. Sandstrom, Academic Press, London, 1982. *(b)* M. L. H. Green, L. Wong, *Organometallics,* 1992, **11**, 2660-2668.

24   P. E. Garrou, *Inorg. Chem.*, 1975, **14**, 1435-39

25   SAINT+, version 6.01: Area-Detector Integration Software, Bruker AXS, Madison 2001.

26   SADABS 2016/02. L. Krause, R. Herbst-Irmer, G. M. Sheldrick, D. Stalke, *J. Appl. Crystallogr.,* 2015, **48**, 3-10.

27   *(a)* G. M. Sheldrick, *Acta Crystallogr. A,* 1990, **46**, 467-473. *(b)* G. M. Sheldrick, *Acta Crystallogr. A,* 2008, **64**, 112-122.

28   G. M. Sheldrick, *Acta Crystallogr. C,* 2015, **71**, 3-8.

29   L. J. Farrugia, *J. Appl. Crystallogr.,* 2012, **45**, 849-854.

30   P. vd. Sluis, L. Spek, *Acta Crystallogr. A,* 1990, **46**, 194-201.

31   G. M. Sheldrick, 1996, Cell_now program (version 2008-2), University of Göttingen, Germany.

32   TwinAbs: Bruker AXS scaling for twinned crystals (version 2008-2), Bruker AXS, Madison 2001.

33   M. J. Frisch, G. W. Trucks, H. B. Schlegel, G. E. Scuseria, M. A. Robb, J. R. Cheeseman, G. Scalmani, V. Barone, B. Mennucci, G. A. Petersson, H. Nakatsuji, M. Caricato, X. Li, H. P. Hratchian, A. F. Izmaylov, J. Bloino, G. Zheng, J. L. Sonnenberg, M. Had, 2009. Gaussian 09, Revision D.01.

34   (*a*) C. Lee, W. Yang, R. G. Parr, *Phys. Rev. B*, 1988, **37**, 785-789. (*b*) A. D. Becke, *J. Chem. Phys*., 1993, **98**, 1372-1377. (*c*) A. D. Becke, *J. Chem. Phys*., 1993, **98**, 5648-5652. (*d*) S. Grimme, J. Antony, S. Ehrlich, H. Krieg, *J. Chem. Phys*., 2010, **132**, 154104.